ChemComm



COMMUNICATION

View Article Online
View Journal | View Issue



A four-state fluorescent molecular switch†

Cite this: Chem. Commun., 2018, 54, 12041

Received 27th June 2018, Accepted 27th September 2018

DOI: 10.1039/c8cc05159c

rsc.li/chemcomm

Yuan Liu, \mathbb{D}^a Jiawang Zhou, \mathbb{D}^{ab} Michael R. Wasielewski, \mathbb{D}^{ab} Hang Xing \mathbb{D}^{*ac} and Chad A. Mirkin \mathbb{D}^{*a}

Four distinct fluorescent states are achieved in a single Weak-Link Approach (WLA) construct bearing pyrene and tetraphenylethene moieties. The fluorescence of the compound in both the solution and solid phases can be manipulated through reversible coordination chemistry at the Pt^{II} center.

Stimuli-responsive molecules and materials with tunable photoluminescence properties integrate target recognition and signal transduction processes, and thus, can be useful for the development of sensing and imaging techniques.¹⁻⁶ Moreover, the incorporation of multiple responsive and signalling motifs into one structure enables the detection of different stimuli within one system, thereby expanding their potential utility. However, the design of multi-stimuli-responsive photoluminescent systems remains challenging due to interference that can take place between the different fluorescence pathways that are affected by chemical and physical stimuli.⁷⁻⁹ To address this challenge, we introduce a new strategy based on a molecular system where a structural change or phase transition, triggered by different stimuli, can be used to independently and deliberately switch between different fluorescent states. Moreover, in certain cases one can use mixtures of different stimuli to modulate fluorescent states.

Among the ways to construct stimuli-responsive systems, the WLA provides a coordination chemistry-based strategy for the assembly of supramolecular constructs that can be toggled between different coordination states *via* ligand displacements at the transition-metal center using allosteric effectors

(such as small molecules or ions). 10,11 Through synthetic

incorporation of multiple photoluminescent motifs into the

ligands, the changes in coordination modes of the WLA complexes

Herein, we report the first example of heteroligated Pt" WLA complexes with hemilabile ligands bearing both a conventional (pyrene) and an unconventional fluorophore (tetraphenylethene, TPE). As shown in Fig. 1, in solution, the displacement of the Pt-S bond with an anionic effector, such as Cl⁻ ion, in the pyrene-functionalized phosphino-thioether (P,S) ligand converts the closed complex to the semi-open state, resulting in a "turn-on" fluorescence response of the pyrene due to the distance-dependent heavy atom effect (HAE). 12,19,20 When the solvent polarity is reduced, for instance by the addition of hexane, these complexes precipitate due to reduced solubility, and the pyrene fluorescence is quenched, 21 while the emission of the TPE moiety 222-24 is turned on due to restriction of intramolecular rotation (RIR) in the solid phase. 25,26 In addition, the geometric differences between the semi-open (1) and the closed (2) states also lead to different spectral features in the solid state. In this vein, a four-state fluorescent switch can be realized through the design and synthesis of a single supramolecular construct with orthogonally tuned fluorophores.

Our design of the (P,S) hemilabile ligands was motivated by the hypothesis that a heteroligated WLA complex can be assembled into a semi-open state from a Pt^{II} metal precursor and two (P,S) ligands with different sulfur atom electron donating abilities.²⁷ Based on this hypothesis, we designed, synthesized, and characterized the hemilabile ligand 3 with an electronwithdrawing phenylene spacer between the pyrene and sulphur

result in different fluorescence outputs, such as emission intensity, fluorescence lifetimes, and emission spectral features. ¹² Based upon these changes in fluorescence properties, WLA assemblies have been exploited as fluorescent probes, ¹² photoredox switches, ¹³ and light-harvesting arrays. ^{14,15} We hypothesized that by incorporating a pair of fluorescent motifs with different emission mechanisms into the WLA assembly, changes in the coordination or phase state of the WLA complex triggered by different chemical stimuli could tune the fluorescent profile of these two fluorophores orthogonally, leading to multiple fluorescence outputs.

Herein, we report the first example of heteroligated Pt^{II} WLA complexes with hemilabile ligands bearing both a conventional (pyrene) and an unconventional fluorophore (tetraphenylethene, TPE). ^{16–18} As shown in Fig. 1, in solution, the displacement of

^a Department of Chemistry and International Institute for Nanotechnology, Northwestern University, 2145 Sheridan Road, Evanston, Illinois 60208, USA. E-mail: chadnano@northwestern.edu, hangxing@hnu.edu.cn

b Institute for Sustainability and Energy at Northwestern, Northwestern University, Evanston, Illinois 60208, USA

^c Institute of Chemical Biology and Nanomedicine, State Key Laboratory for Chemo/Bio Sensing and Chemometrics, College of Chemistry and Chemical Engineering, Hunan University, Changsha, Hunan 410082, China

 $[\]dagger$ Electronic supplementary information (ESI) available: Synthesis, HR-MS, NMR spectra, computational results, and optical data. See DOI: 10.1039/c8cc05159c

Communication ChemComm

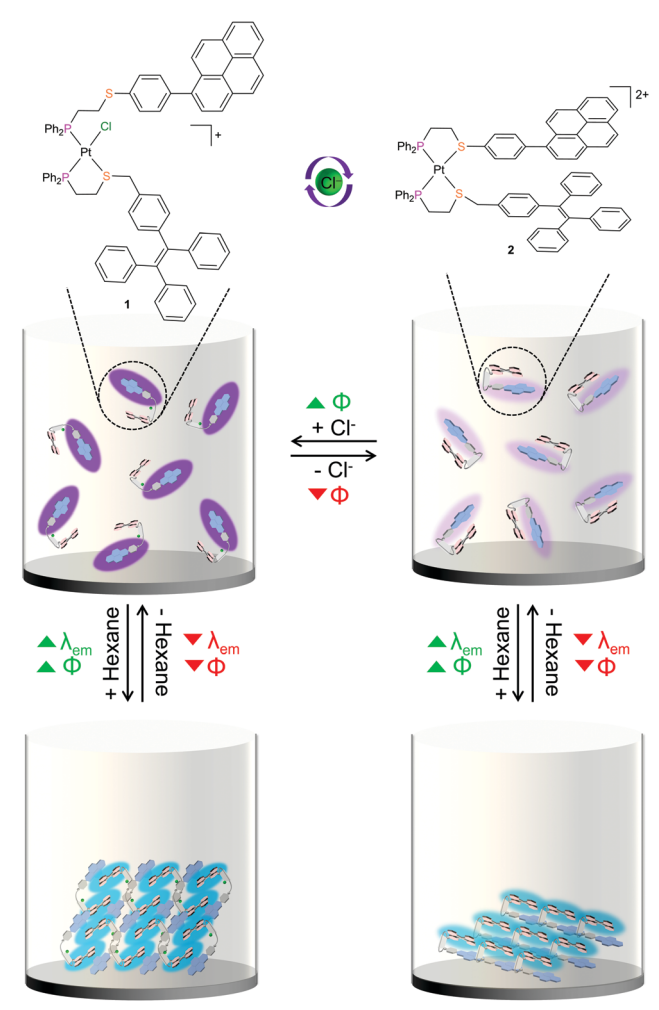


Fig. 1 Modulation of fluorescence properties via a coordinationchemistry based system. Four distinct fluorescent states can be achieved with this WLA system via the change of coordination states of the complexes (left column: semi-open vs. right column: closed) and change between solution (top row) and solid states (bottom row). λ_{em} : wavelength of maximum fluorescence emission. Φ : quantum yield of fluorescence emission. Arrows indicate an increase or decrease in λ_{em} and \varPhi upon changing state. Counterions have been omitted for clarity.

atom, and ligand 4, which possesses an electron-donating methylene spacer between the TPE and sulfur atom (see Scheme S1, ESI†). These two ligands were characterized by ¹H and ³¹P NMR spectroscopy as well as high-resolution mass spectrometry (HR-MS) (see ESI†).

The heteroligated semi-open complex 1 was prepared via sequential addition of ligands 3 and 4 to a dichloromethane (DCM) solution of dicholoro(1,4-cyclooctadiene)platinum(II) [Pt(cod)Cl₂] at room temperature (Scheme 1). The formation of semi-open complex 1 was confirmed by HR-MS and two diagnostic sets of ³¹P{¹H} NMR resonances arising from the P-bound ligand 3 (δ 8.6 ppm, J_{P-P} = 14 Hz, J_{P-Pt} = 3171 Hz) and chelated ligand 4 (δ 42.6 ppm, J_{P-P} = 14 Hz, J_{P-Pt} = 3500 Hz).²⁸ The semi-open complex 1 was quantitatively converted into the closed form 2 via the extraction of Cl with silver tetrafluoroborate (AgBF₄), as evidenced by the diagnostic ³¹P{¹H} NMR

resonances of the two non-equivalent chelated phosphine ligands (δ 44.6 ppm, J_{P-P} = 12 Hz, J_{P-Pt} = 3129 Hz; δ 46.3 ppm, $J_{P-P} = 12 \text{ Hz}, J_{P-Pt} = 3105 \text{ Hz}).^{28} \text{ The closed complex 2 can be}$ converted back to the semi-open form 1 by the addition of tetrabutylammonium chloride (TBACl), illustrating the reversibility of the system.

We next investigated the optical properties of complexes 1 and 2 in both the solution and solid states, using the homoligated complexes bearing only pyrene or TPE moieties for comparison purposes (see Table S1, ESI†). In DCM, both complexes exhibit maximum absorption at 344 nm. Fluorescence measurements determined that the semi-open complex 1 exhibited a much higher quantum yield (10.5%) than the closed complex 2 (0.9%), while the center of the emission peak remains almost unchanged (407 nm for 1 vs. 404 nm for 2, see ESI†). We hypothesize that the significant reduction in quantum yield in the closed complex is due to the HAE. 12,19,20 As reported in previous fluorescent WLA systems, the distance between the heavy PtII center and pyrene moiety is shorter in the closed state than in the semi-open state, which facilitates spin-orbital coupling and quenches the fluorescence. 12,19,20 To verify this hypothesis, we calculated the distances between the PtII center and pyrene moiety in the energy-optimized structures of 1 and 2 using density functional theory (DFT). We found that the Pt-pyrene distance in 2 was 2.5 Å shorter compared to 1, supporting the distance-dependent HAE as the main cause for the decrease of the quantum yield in solution (see Fig. S1, ESI†).

The fluorescence properties of 1 and 2 in the solid phase were then explored. UV irradiation of solids 1 and 2 resulted in stronger fluorescence emission than 1 and 2 in solution with maxima at 475 and 470 nm, respectively. These values are comparable to the reported values for TPE in the literature and the homoligated complex bearing only TPE fluorophores (see Table S1, ESI†). 17,29,30 Notably, a lower quantum yield was observed for solid-state 2 (10.0%) than solid-state 1 (29.8%). The difference in solid-state fluorescence efficiency is attributed to the different packing and out-of-plane distortion of the TPE moiety in the open and closed complexes. In particular, the shorter inter-ligand distance between pyrene and TPE ligands in the closed complex results in inefficient packing and a distorted geometry for TPE, which is known to influence its emission efficiency.^{24,30}

The fluorescence properties of these complexes in both the solution and solid states can be described based upon four distinct emission behaviours (fluorescence maxima and quantum yields). These properties can be observed by studying the in situ fluorescence changes when 2 is converted into 1 in solution, and when 1 and 2 are precipitated from solution. Indeed, when a sub-stoichiometric amount of TBACl is added to a DCM solution of 2, the pyrene emission intensity increases as the closed complex 2 is gradually converted into the semiopen complex 1, consistent with the higher solution quantum yield for 1 compared to 2. The fluorescence emission profile reached a plateau at around 7.5 eq. of TBACl, a consequence of complete outer-sphere counterion exchange (Fig. 2).

ChemComm Communication

Scheme 1 Synthesis of the heteroligated Pt^{II}-WLA complexes from the hemilabile (P,S) ligands with pyrene and TPE moieties

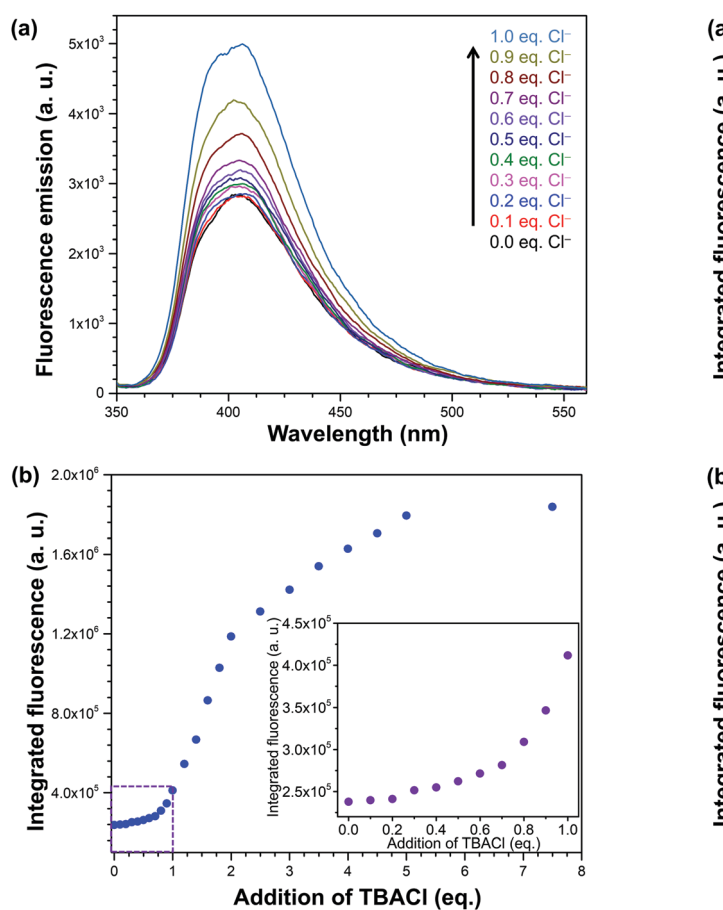
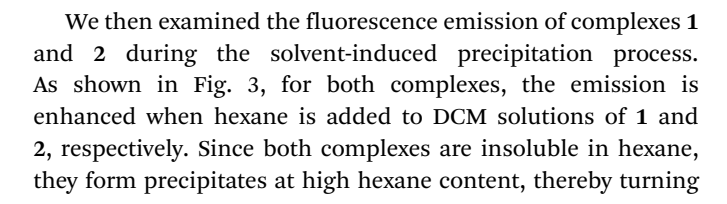


Fig. 2 Addition of TBACl to a DCM solution of 2 (3.8 μ M) results in increased fluorescence emission. Excitation wavelength: 344 nm. (a) Stacked fluorescence spectra of the solution upon addition of (to 1.0 eq.). (b) Plot of integrated fluorescence vs. the addition of TBACl (eq.) to 7.5 eq. Inset: Plot of integrated fluorescence vs. the addition of TBACl (eq.) to 1.0 eq.



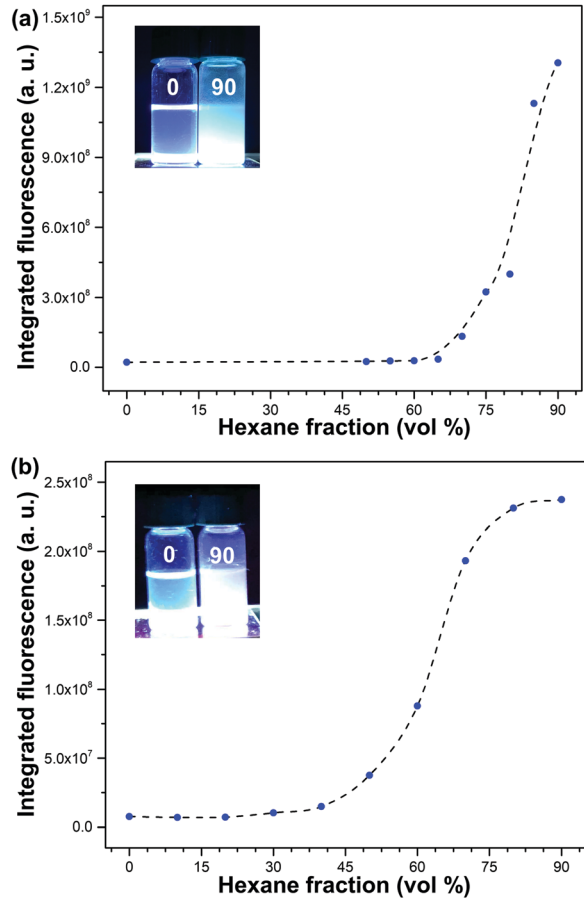


Fig. 3 Plot of integrated fluorescence of the solutions or suspensions of complexes (a) 1 (0.4 mM) and (b) 2 (0.5 mM) in DCM/hexane mixtures vs. hexane fraction (vol%). Inset: Photographs of solutions of complexes (a) 1 and (b) 2 in pure DCM and in a DCM/hexane (90 vol% hexane) mixture taken under UV illumination.

on the fluorescence of the TPE moiety and quenching the fluorescence of the pyrene moiety. Furthermore, a dramatic increase in fluorescence intensity for 1 was observed at 80 vol% of hexane, whereas this increase occurred at ~65 vol% of hexane for 2 (see Fig. S2, ESI†). We attribute the difference to the decreased solubility when the complex was switched from a +1 to +2 state. The structure-property relationship diagram of Communication ChemComm

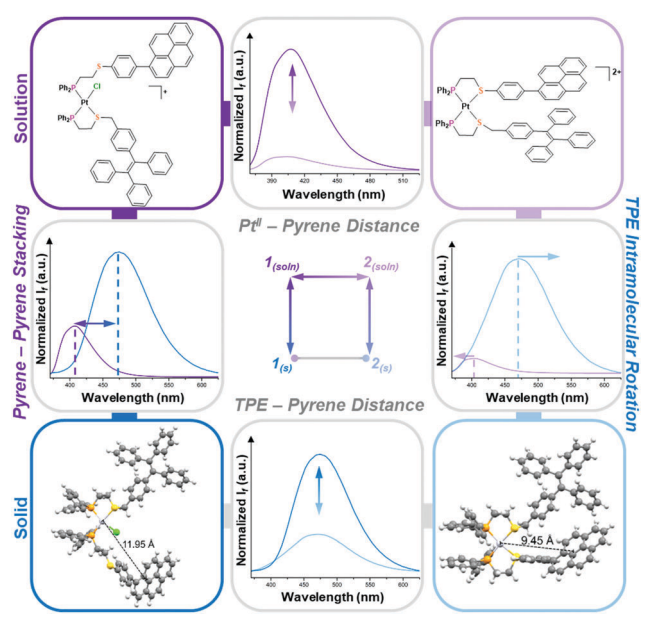


Fig. 4 The four-state photoluminescent molecular switch using WLA coordination complexes. Switching between the solution $[\mathbf{1}_{(\text{soln})} \text{ and } \mathbf{2}_{(\text{soln})}]$ and solid state $[\mathbf{1}_{(\text{s})} \text{ and } \mathbf{2}_{(\text{s})}]$ results in peak shifting and a change in quantum yield, while switching between the semi-open $[\mathbf{1}_{(\text{soln})}]$ and the closed $[\mathbf{2}_{(\text{soln})}]$ coordination states causes changes in quantum yield. Counterions have been omitted for clarity. I_f = fluorescence intensity. Soln = solution. S = solid.

the molecular switch is shown in Fig. 4. The change of fluorescence properties is correlated with the change of the structure of the complex between two states: (1) the quantum yield in solution is related to the Pt^{II}-pyrene distance; (2) the quantum yield in the solid state is related to the inter-ligand distance; and (3) the peak shift during the solution-to-solid transition is related to the relative contribution from TPE and pyrene emission.

In summary, we have reported a multi-stimuli-responsive WLA system with four distinct fluorescence outputs. Different chemical stimuli (Cl⁻ or hexane) independently trigger a structure change or phase transition for this WLA assembly, which results in a modulation of the fluorescent profiles of the pyrene and TPE motifs. This present work expands the scope of fluorescent WLA systems and provides a novel coordination chemistry-based approach for the design of multi-stimuli-responsive photoluminescent systems. These constructs will be useful for the development of novel sensing and imaging techniques.

This material is based on work supported by the following awards: National Science Foundation grant CHE-1709888, Sherman Fairchild Foundation, U.S. Army grant W911NF-15-1-0151, Air Force Research Laboratory award FA8650-15-2-5518, and National Cancer Institute of the National Institutes of Health award U54CA199091 (C. A. M.), and Chemical Sciences, Geosciences, and Biosciences Division, Office of Basic Energy Sciences, DOE under grant no. DE-FG02-99ER14999 (M. R. W.). The content is solely the responsibility of the authors and does not necessarily represent the official views of the National Institutes of Health, the Air Force Research Laboratory, or the U.S. Government. The U.S. Government is

authorized to reproduce and distribute reprints for Governmental purposes notwithstanding any copyright notation thereon.

Conflicts of interest

There are no conflicts to declare.

Notes and references

- N. Yanai, K. Kitayama, Y. Hijikata, H. Sato, R. Matsuda, Y. Kubota, M. Takata, M. Mizuno, T. Uemura and S. Kitagawa, *Nat. Mater.*, 2011, 10, 787.
- 2 Z. G. Chi, X. Q. Zhang, B. J. Xu, X. Zhou, C. P. Ma, Y. Zhang, S. W. Liu and J. R. Xu, *Chem. Soc. Rev.*, 2012, 41, 3878.
- 3 Y. Chen, W. Zhang, Z. Zhao, Y. Cai, J. Gong, R. T. K. Kwok, J. W. Y. Lam, H. H. Y. Sung, I. D. Williams and B. Z. Tang, *Angew. Chem., Int. Ed. Engl.*, 2018, 57, 5011.
- 4 L. Chen, J. W. Ye, H. P. Wang, M. Pan, S. Y. Yin, Z. W. Wei, L. Y. Zhang, K. Wu, Y. N. Fan and C. Y. Su, *Nat. Commun.*, 2017, 8, 15985.
- 5 V. K. Outlaw, J. Zhou, A. E. Bragg and C. A. Townsend, RSC Adv., 2016, 6, 61249.
- 6 J. Zhou, V. K. Outlaw, C. A. Townsend and A. E. Bragg, *Chem. Eur. J.*, 2016. 22, 15212.
- 7 A. J. McConnell, C. S. Wood, P. P. Neelakandan and J. R. Nitschke, Chem. Rev., 2015, 115, 7729.
- 8 S. Perruchas, X. F. Le Goff, S. Maron, I. Maurin, F. Guillen, A. Garcia, T. Gacoin and J. P. Boilot, *J. Am. Chem. Soc.*, 2010, **132**, 10967.
- 9 H.-S. Tang, N. Zhu and V. W.-W. Yam, Organometallics, 2007, 26, 22.
- 10 A. M. Lifschitz, M. S. Rosen, C. M. McGuirk and C. A. Mirkin, J. Am. Chem. Soc., 2015, 137, 7252.
- 11 B. J. Holliday and C. A. Mirkin, Angew. Chem., Int. Ed., 2001, 40, 2022.
- 12 A. M. Lifschitz, C. M. Shade, A. M. Spokoyny, J. Mendez-Arroyo, C. L. Stern, A. A. Sarjeant and C. A. Mirkin, *Inorg. Chem.*, 2013, 52, 5484.
- 13 A. M. Lifschitz, R. M. Young, J. Mendez-Arroyo, V. V. Roznyatovskiy, C. M. McGuirk, M. R. Wasielewski and C. A. Mirkin, *Chem. Commun.*, 2014, 50, 6850.
- 14 A. M. Lifschitz, R. M. Young, J. Mendez-Arroyo, C. L. Stern, C. M. McGuirk, M. R. Wasielewski and C. A. Mirkin, *Nat. Commun.*, 2015, 6, 6541.
- 15 A. M. Lifschitz, R. M. Young, J. Mendez-Arroyo, C. M. McGuirk, M. R. Wasielewski and C. A. Mirkin, *Inorg. Chem.*, 2016, 55, 8301.
- 16 D. Ding, K. Li, B. Liu and B. Z. Tang, Acc. Chem. Res., 2013, 46, 2441.
- 17 X. Z. Yan, T. R. Cook, P. Wang, F. H. Huang and P. J. Stang, Nat. Chem., 2015, 7, 342.
- 18 M. Zhang, S. Yin, J. Zhang, Z. Zhou, M. L. Saha, C. Lu and P. J. Stang, Proc. Natl. Acad. Sci. U. S. A., 2017, 114, 3044.
- 19 S. K. Lower and M. A. El-Sayed, Chem. Rev., 1966, 66, 199.
- 20 M. A. Elsayed, Acc. Chem. Res., 1968, 1, 8.
- 21 S. A. Jenekhe and J. A. Osaheni, Science, 1994, 265, 765.
- 22 J. D. Luo, Z. L. Xie, J. W. Y. Lam, L. Cheng, H. Y. Chen, C. F. Qiu, H. S. Kwok, X. W. Zhan, Y. Q. Liu, D. B. Zhu and B. Z. Tang, *Chem. Commun.*, 2001, 1740.
- 23 Y. Hong, J. W. Lam and B. Z. Tang, Chem. Soc. Rev., 2011, 40, 5361.
- 24 J. Mei, N. L. C. Leung, R. T. K. Kwok, J. W. Y. Lam and B. Z. Tang, Chem. Rev., 2015, 115, 11718.
- 25 Y. N. Hong, J. W. Y. Lam and B. Z. Tang, Chem. Commun., 2009, 4332.
- 26 J. Mei, Y. N. Hong, J. W. Y. Lam, A. J. Qin, Y. H. Tang and B. Z. Tang, Adv. Mater., 2014, 26, 5429.
- 27 C. G. Oliveri, P. A. Ulmann, M. J. Wiester and C. A. Mirkin, Acc. Chem. Res., 2008, 41, 1618.
- 28 P. E. Garrou, Chem. Rev., 1981, 81, 229.
- 29 W. Z. Yuan, P. Lu, S. Chen, J. W. Lam, Z. Wang, Y. Liu, H. S. Kwok, Y. Ma and B. Z. Tang, Adv. Mater., 2010, 22, 2159.
- 30 Z. J. Zhao, P. Lu, J. W. Y. Lam, Z. M. Wang, C. Y. K. Chan, H. H. Y. Sung, I. D. Williams, Y. G. Ma and B. Z. Tang, *Chem. Sci.*, 2011, 2, 672.

Electronic Supplementary Information

A Four-State Fluorescent Molecular Switch

Yuan Liu,^a Jiawang Zhou,^{ac} Michael R. Wasielewski, ^{ac} Hang Xing, ^{*ab} and Chad A. Mirkin^{*a}

*To whom correspondence should be addressed,

E-mail: chadnano@northwestern.edu; hangxing@hnu.edu.cn.

^a Department of Chemistry and International Institute for Nanotechnology, Northwestern
 University, 2145 Sheridan Road, Evanston, Illinois 60208, USA
 ^b Institute of Chemical Biology and Nanomedicine, Molecular Science and Biomedicine
 Laboratory, State Key Laboratory for Chemo/Bio Sensing and Chemometrics, College of
 Chemistry and Chemical Engineering, Hunan University, Changsha, Hunan 410082, China
 ^c Institute for Sustainability and Energy at Northwestern, Northwestern University, Evanston,
 Illinois 60208, USA

Table of Contents

Experimental	(S3)
Scheme S1. Syntheses of (P,S)-Ligands with Pyrene and TPE Moieties	
Scheme S2. Syntheses of Homoligated Complexes S1, S2 and S3	
Table S1. Optical Properties of Complexes 1, 2, S1, S2 and S3	(S9)
Fig. S1. Calculated Structures of 1 and 2	(S10)
Fig. S2. Photographs and Fluorescence Spectra of Solutions or Suspensions of 1 and 2	(S11)
Absorption Spectra	(S12)
Fluorescence Spectra	(S18)
Mass Spectra	(S27)
NMR Spectra	(S31)
References	(S40)

Experimental

Materials and Methods. 1-[(4-Bromomethyl)phenyl]-1,2,2-triphenylethene (9)¹ and 1-chloro-2-diphenylphosphinoethane² were prepared according to modified literature procedures. All other chemicals and anhydrous solvents were purchased from Sigma-Aldrich and used as received. Deuterated solvents were purchased from Cambridge Isotope Laboratories and used as received. All NMR spectra were recorded on a Bruker Advance 400 MHz spectrometer, a Bruker Advance III 500 MHz spectrometer, and an Agilent DD2 500 MHz spectrometer. ¹H NMR spectra were referenced to residual protons in the deuterated solvents [CDCl₃, δ 7.26; CD₂Cl₂, δ 5.32; (CD₃)₂SO, δ 2.50] internally. ¹³C NMR spectra were referenced to residual carbons in the deuterated solvents (CDCl₃, δ 77.16) internally. Atmospheric pressure photoionization (APPI) and electrospray ionization (ESI) mass spectrometry (MS) spectra were recorded on a Bruker Impact-II in positive-ion mode and an Agilent 6210 LC-TOF in positive-ion mode, respectively.

UV-vis absorption measurements were performed on a Shimadzu UV-1800 spectrophotometer using a 10 mm cell-path quartz cuvette (VMR). Fluorescence emission measurements were acquired using HORIBA Nanolog spectrofluorimeter equipped with a 450-W Xe lamp excitation source and a photomultiplier tube (PMT) detector. The spectra were corrected for the monochromator wavelength dependence and photomultiplier response functions provided by the manufacturer. The widths for either the entrance or exit slits were less than 5 nm. Absolute photoluminescence quantum yields of both solution and solid states were determined using an integrating sphere (Horiba Quanta–φ). For solution samples, the spectra of solvent blank were first measured with the entrance and exit slits adjusted to make the pump scatter intensity less than 2×10^6 counts at the excitation wavelength. With the same entrance and exit slits, the spectra of the sample solutions were measured under highly diluted conditions (optical density less than 0.1) to avoid self-absorption. Then, the fluorescence quantum yields and the absolute errors of the measurements were calculated using the 2-curve analysis, in which the Rayleigh line and luminescence band were included together in the sample's and blank's data with the "Quantaphi LiquidCorrect 695" as the sphere correction method. For solid samples, the spectra of the solid blank [a powder cup with a quartz coverslip purchased from HORIBA Scientific (item # 5500000064)] were first measured with the entrance or exit slits adjusted to make the pump scatter intensity less than 2×10^6 counts at the excitation wavelength. Then, the DCM solutions of samples were drop-casted on the powder cup with a quartz coverslip and inserted into the integration sphere. Under the same conditions as the solid blank, the spectra of the solid samples were measured, and the fluorescence quantum yields and the absolute errors of the measurements were calculated using the 2-curve analysis, in which the Rayleigh line and luminescence band are included together in the sample's and blank's data with the "Quanta-phi SolidCorrect 695" as the sphere correction method. All spectra were plotted using Origin (OriginLab) and were smoothed using the built-in adjacent-averaging method with a 10-point window.

DFT calculations were made using the Amsterdam Density Functional (ADF2017.111) suite³⁻⁵ on a 16-core computational cluster. Geometry optimizations were made without restraint in the ADF GUI using basis sets containing triple-ζ functions with two polarization function (TZ2P),⁶ and the local density approximations of Generalized Gradient Approximation: Perdew-Burke-Ernzerhof (GGA:PBE).⁷

Synthesis. *1-(4-Thiomethylphenyl)-pyrene* (6). 1-Bromopyrene (281 mg, 1.00 mmol), 4-(thiomethyl)phenylboronic acid (185 mg, 1.10 mmol), Pd(dppf)Cl₂·CH₂Cl₂ (41 mg, 0.05 mmol), and Na₂CO₃ (318 mg, 3.00 mmol) were added into a mixture of 1,2-dimethoxyethane (DME)/H₂O

(10 mL, DME/H₂O = 3/1) under N₂. The resulting mixture was refluxed at 95 °C for 16 hours, and the reaction was quenched with 1.0 M HCl solution at room temperature, at which time the precipitates were observed and removed by filtration. The filtrate was extracted with Et₂O (3 x 10 mL), washed with brine, and dried over MgSO₄. The solvent was removed under reduced pressure, and the resulting residue was purified by flash column chromatography on silica gel (Hexane/ethyl acetate = 100/1) to afford the desired product **6** in 73% yield (237 mg, 0.73 mmol). ¹H NMR (500 MHz, CDCl₃): δ 8.23–8.16 (m, 4H), 8.10 (s, 2H), 8.04–7.96 (m, 3H), 7.57 (d, J = 8.4 Hz, 2H), 7.46 (d, J = 8.3 Hz, 2H), 2.61 (s, 3H). ¹³C NMR (126 MHz, CDCl₃): δ 138.12, 137.76, 137.25, 131.65, 131.16, 131.13, 130.75, 128.65, 127.67, 127.59, 127.56, 126.63, 126.19, 125.32, 125.29, 125.15, 125.07, 125.00, 124.83, 16.06.

1-(4-Thiophenyl)-pyrene (5). Compound 6 (100 mg, 0.31 mmol) and sodium ethanethiolate (90%, 145 mg, 1.55 mmol) were added to DMF (2 mL) N₂. The resulting mixture was refluxed at 155 °C overnight, and the reaction was quenched with 1.0 M HCl solution at room temperature, at which time yellow precipitates were formed. The mixture was extracted with Et₂O (3 x 10 mL), washed with H₂O (2 x 10 mL) and brine, and dried over MgSO₄. The solvent was removed under reduced pressure to afford yellow solid as the crude product 5 in 97% yield (93 mg, 0.30 mmol), which was confirmed by ¹H NMR and carried to next step without purification. ¹H NMR (500 MHz, CDCl₃): δ 8.22–8.14 (m, 4H), 8.10 (s, 2H), 8.04–8.00 (m, 2H), 7.94 (d, J = 7.8 Hz, 1H), 7.52 (d, J = 8.3 Hz, 2H), 7.48 (d, J = 8.4 Hz, 2H).

(*P,S*)-*Pyrene* (*3*). Compound **5** (93 mg, 0.30 mmol), 1-chloro-2-diphenylphosphinoethane (81 mg, 0.33 mmol), and Cs₂CO₃ (111 mg, 0.34 mmol) were stirred in MeCN (4 mL). The resulting mixture was refluxed at 82 °C for 15 hours, at which time the solvent was removed under reduced pressure. The resulting residue was purified by flash column chromatography on silica gel (Hexane/ ethyl acetate = 95/5) to afford the desired ligand **3** in 72% yield (116 mg, 0.22 mmol). ¹H NMR (500 MHz, CD₂Cl₂): δ 8.25–8.16 (m, 5H), 8.12 (s, 2H), 8.06–8.02 (m, 2H), 7.97 (d, J = 7.8 Hz, 1H), 7.54 (d, J = 8.3 Hz, 2H), 7.48–7.44 (m, 4H), 7.41 (d, J = 8.2 Hz, 2H), 7.39–7.35 (m, 5H), 3.11–3.07 (m, 2H), 2.51–2.47 (m, 2H). ³¹P{¹H} NMR (202 MHz, CD₂Cl₂): δ -17.24. HRMS (APPI+): m/z calcd for C₃₆H₂₇PS [M]⁺: 522.1566; found: 522.1556.

1-[(4-S-Methyl thiourea)phenyl]-1,2,2-triphenylethene (8). 1-[(4-Bromomethyl)phenyl]-1,2,2-triphenylethene (9) (100 mg, 0.24 mmol) and thiourea (21 mg, 0.28 mmol) were added to ethanol (3 mL) under N₂. The resulting mixture were refluxed at 80 °C for 4 hours and cooled to room temperature. The solution was concentrated under reduced pressure, and hexane (10 mL) was added to initiate precipitation. The precipitates were filtered and washed with hexane (3 x 10 mL) to afford white solid as the crude product 8 in 85% yield (100 mg, 0.2 mmol), which was confirmed by 1 H NMR and carried to next step without purification. 1 H NMR (500 MHz, DMSO- d_6): δ 9.11–8.94 (m, 4H), 7.17–7.10 (m, 11H), 6.98–6.95 (m, 8H), 4.38 (s, 2H).

1-[(4-methylthiol)phenyl]-1,2,2-triphenylethene (7). Compound **8** (100 mg, 0.2 mmol) was dissolved in a mixture of ethanol/H₂O (6 mL, Ethanol/H₂O = 3/1), and the resulting solution was saturated with N₂ for 20 min before 1.0 M solution of sodium hydroxide (9.6 mg, 0.24 mmol) was added. The reaction mixture was heated to 70 °C under N₂ for 5 hours, at which time the reaction was cooled to room temperature and quenched with saturated ammonium chloride solution until the pH of the solution reached about 6.5. The resulting mixture was extracted with CH₂Cl₂ (3 x 20 mL), washed with brine, and dried over Na₂SO₄. The solvent was removed under reduced pressure to afford light yellow solid as the crude product **7** in 91% yield (69 mg, 0.181 mmol), which was

confirmed by 1 H NMR and carried to next step without purification. 1 H NMR (500 MHz, CDCl₃): δ 7.11–7.08 (m, 9H), 7.06–7.00 (m, 8H), 6.97–6.96 (m, 2H), 3.65 (d, J = 7.5 Hz, 2H).

(*P,S*)-*TPE* (4). Compound 7 (100 mg, 0.26 mmol) and potassium tert-butoxide (31 mg, 0.28 mmol) were stirred in MeCN (10 mL) at room temperature for 15 min before 1-chloro-2-diphenylphosphinoethane (62 mg, 0.25 mmol) was added. The resulting mixture was refluxed at 82 °C for 15 hours, at which time the solvent was removed under reduced pressure. The resulting residue was purified by flash column chromatography on silica gel (Hexane/ethyl acetate = 95/5) to afford the desired ligand 4 in 79.5% yield (118 mg, 0.20 mmol). ¹H NMR (400 MHz, CD₂Cl₂): δ 7.42–7.37 (m, 3H), 7.34–7.32 (m, 5H), 7.11–7.07 (m, 10H), 7.03–7.01 (m, 7H), 6.95–6.90 (m, 4H), 3.60 (s, 2H), 2.47–2.41 (m, 2H), 2.31–2.27 (m, 2H). ³¹P{¹H} NMR (162 MHz, CD₂Cl₂): δ -16.79. HRMS (APPI+): m/z calcd for C₄₁H₃₆PS [M+H]⁺: 591.2270; found: 591.2255.

Semi-open complex (1). A solution of (P,S)-TPE (4) (8 mg, 0.014 mmol) in 1 mL of CH₂Cl₂ was added dropwise to a solution of dichloro(1,4-cyclooctadiene)platinum-(II) (5 mg, 0.014 mmol) in 1 mL of CH₂Cl₂. The solution was stirred at room temperature for 5 min, and a solution of (P,S)-pyrene (3) (7 mg, 0.014 mmol) in 1 mL of CH₂Cl₂ was added. The resulting mixture was stirred for additional 30 min. The solution was then concentrated under reduced pressure, and hexane (10 mL) was added to initiate precipitation. The precipitates were filtered and washed with hexane (3 x 10 mL) to afford light yellow solid as the product 1 in >95% yield (20 mg, 0.014 mmol). ¹H NMR (400 MHz, CD₂Cl₂): δ 8.26–7.94 (m, 9H), 7.53–7.27 (m, 25H), 7.09–6.96 (m, 18H), 3.16–3.10 (m, 2H), 2.84–2.78 (m, 2H), 2.44 (br, 1H), 1.91 (br, 1H), 1.26 (s, 2H), 0.89–0.83 (m, 2H). ³¹P{¹H} NMR (162 MHz, CD₂Cl₂): 42.6 (d, J_{P-P} = 14 Hz, J_{P-Pt} = 3500 Hz, 1P), 8.6 (d, J_{P-P} = 14 Hz, J_{P-Pt} = 3171 Hz, 1P). HRMS (ESI+): m/z calcd for C₇₇H₆₂P₂S₂Pt [M-Cl]⁺: 1342.310; found: 1342.311.

Fully closed complex (2). Semi-open complex 1 (20 mg, 0.014 mmol) and silver tetrafluoroborate (8.6 mg, 0.028 mmol) were mixed in CH₂Cl₂ (1 mL). The resulting mixture was stirred at room temperature for 20 min in the absence of light. The mixture was then filtered, and the filtrate was dried under reduced pressure to afford the desired product 2 as a yellow solid in >95% yield (21 mg, 0.014 mmol). ¹H NMR (400 MHz, CD₂Cl₂): δ 8.27–7.81 (m, 13H), 7.53 (br, 20H), 7.09–6.91 (m, 19H), 3.18 (br, 4H), 1.27 (s, 4H), 0.90–0.83 (m, 2H). ³¹P{¹H} NMR (162 MHz, CD₂Cl₂): δ 46.3 (d, J_{P-P} = 12 Hz, J_{P-Pt} = 3105 Hz, 1P), 44.6 (d, J_{P-P} = 12 Hz, J_{P-Pt} = 3129 Hz, 1P). HRMS (ESI+): m/z calcd for C₇₇H₆₂P₂S₂BF₄Pt [M-BF₄]⁺: 1394.344; found: 1394.345.

Procedure. Tritration experiment for Figure 2. A DCM solution (2.5 mL) of the fully closed complex **2** (3.8 μM) was added to the cuvette at room temperature. The fluorescence measurement of this solution was recorded as the first data point (0.0 eq. of TBACl). Then, 5 μL of a DCM solution of TBACl (200 μM) was added to the cuvette, providing 0.1 eq. of Cl⁻ ion with respect to complex **2**. The resulting mixture was shaken gently, and the fluorescence was measured. This procedure was repeated for 10 times until 1.0 eq. of Cl⁻ was added to the cuvette. 10 μL of a DCM solution of TBACl (200 μM) was next added to the cuvette, providing 0.2 eq. of Cl⁻ ion with respect to complex **2**, and the fluorescence was recorded following the aforementioned procedures. Upon the addition of 2.0 eq. of TBACl, 25 μL of a DCM solution of TBACl (200 μM) was added to the cuvette, providing 0.5 eq. of Cl⁻ ion. Then, the fluorescence was recorded following the aforementioned procedure until 4.5 eq. of TBACl was added. Finally, 50 μL and 100 μL of a DCM solution of TBACl (200 μM) were added sequentially, and the fluorescence measurement of the solution was recorded as the data points for 5.5 eq. and 7.5 eq. of TBACl, respectively.

Fluorescence measurements for Figure 3 and Figure S2. The DCM solution (2.5 mL) of complexes 1 (4 mM) and 2 (5 mM) are prepared at room temperature as the stock solution. To each vial was added 0.1 mL of the stock solution, and then, different amount of DCM and hexane was added to make 1 mL of the final volume with various hexane fraction (0 vol% to 90 vol%). For the measurement, the solutions or the suspensions were transferred to the cuvette with a stir bar at the bottom, and the fluorescence was recorded with gentle stirring.

Syntheses of (P,S)-Ligands

Scheme S1. Syntheses of (P,S)-ligands with pyrene and TPE moieties

Synthesis of Homoligated Complexes

Scheme S2. (a) Syntheses of the homoligated Pt^{II} -WLA complexes **S1** and **S2** from (P,S)-pyrene ligand **3**. (b) Syntheses of the homoligated Pt^{II} -WLA complexes **S3** from (P,S)-TPE ligand **4**.

Table for Optical Properties

Table S1. Optical properties^a of complexes 1, 2, S1, S2 and S3 in solution^b and solid^c states

Compound, State	λ _{em} (nm)	Quantum Yield, Φ (%)
1, solution	407	10.5 (± 0.15)
1, solid	475	$29.8 \ (\pm \ 0.10)$
2, solution	404	$0.9 \ (\pm \ 0.13)$
2, solid	470	$10.0 \ (\pm \ 0.03)$
S1, solution	391	$1.9 \ (\pm \ 0.27)$
S2, solution	386	$\mathbf{N}\mathbf{A}^d$
S3, solid	481	$15.2 \ (\pm \ 0.02)$

^a Excitation wavelength: 344 nm for 1, 2, S1, and S2; 311 nm for S3. ^b In DCM solution at room temperature. Concentration: 1 (3.4 μM), 2 (3.5 μM), S1 (1.6 μM), and S2 (1.4 μM). ^c Solid samples drop-casted on powder cups with a quartz coverslip. ^d No measurable quantum yields were recorded for S2 in solution.

Energy minimized DFT Models of Complex 1 and 2

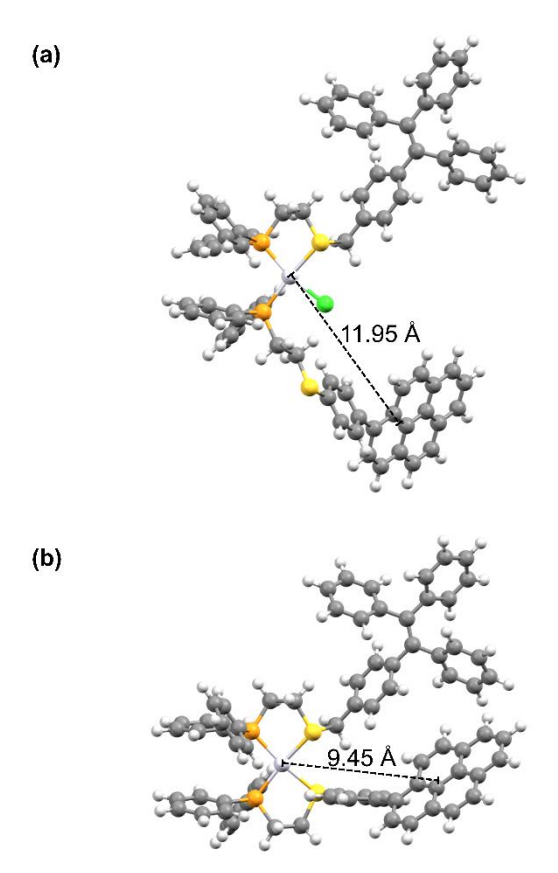


Fig. S1. Calculated structures of (a) 1 and (b) 2. The distances were measured between the Pt^{II} center and the center of the pyrene moiety. Counterions have been omitted for clarity.

Photographs and Fluorescence Spectra of Solutions or Suspensions of 1 and 2

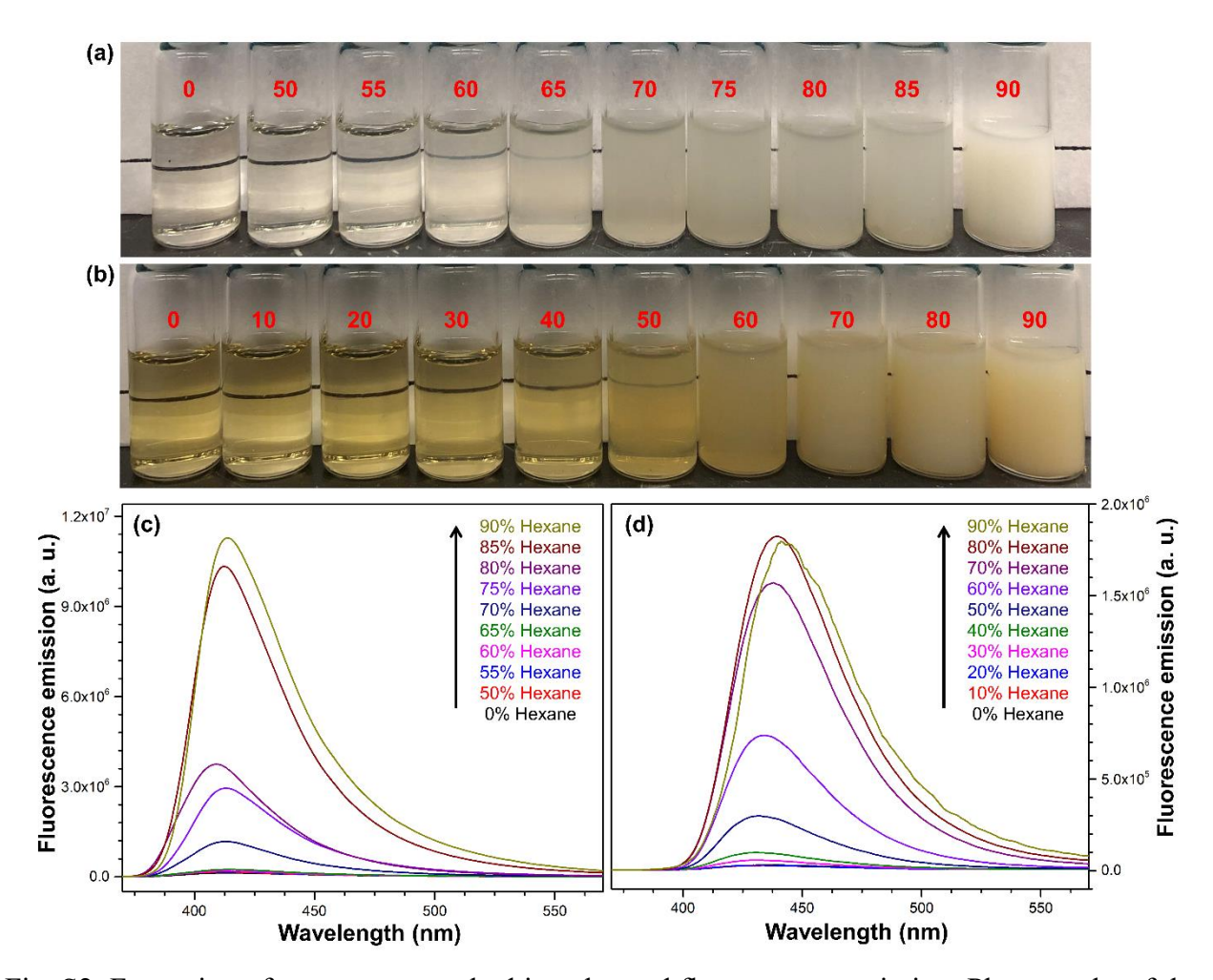
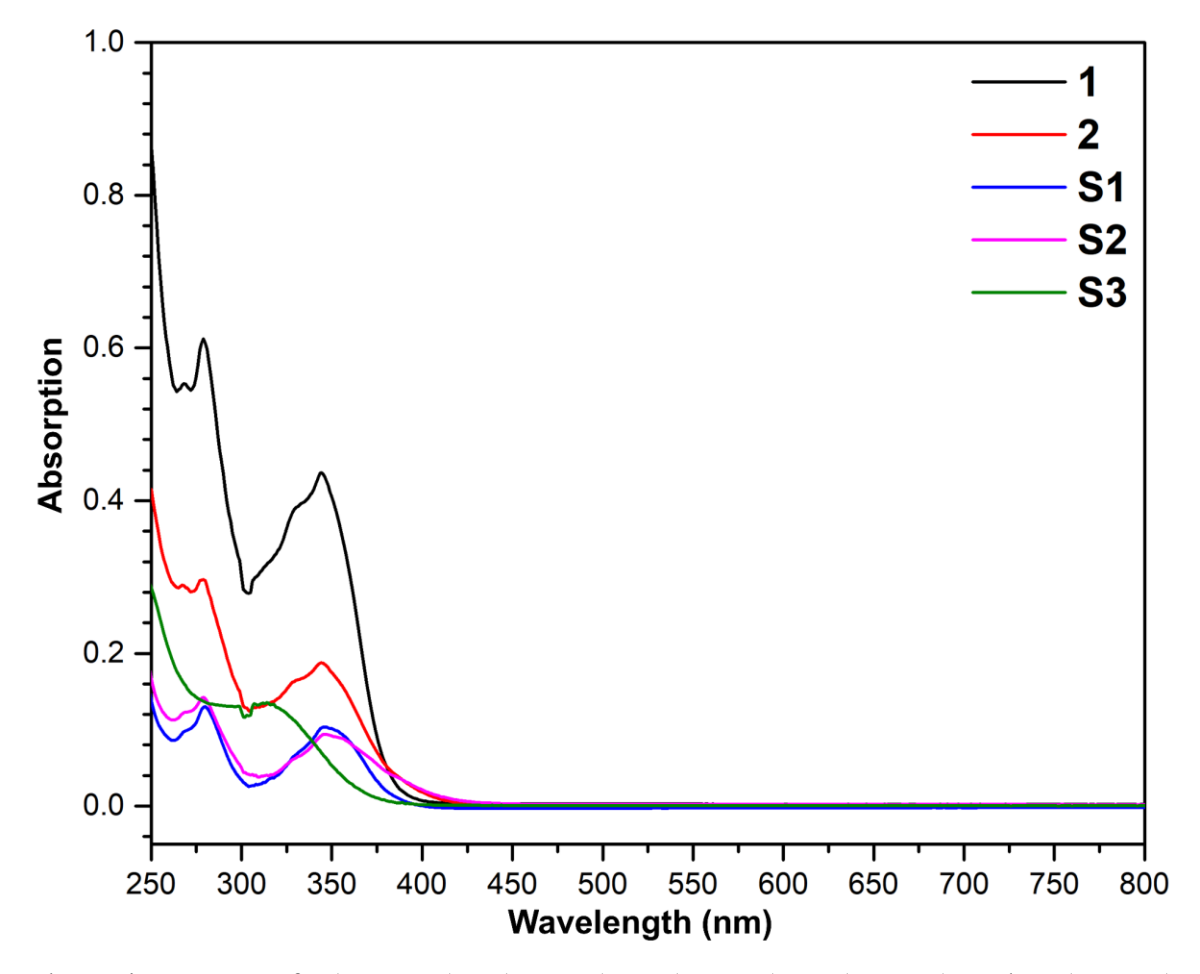
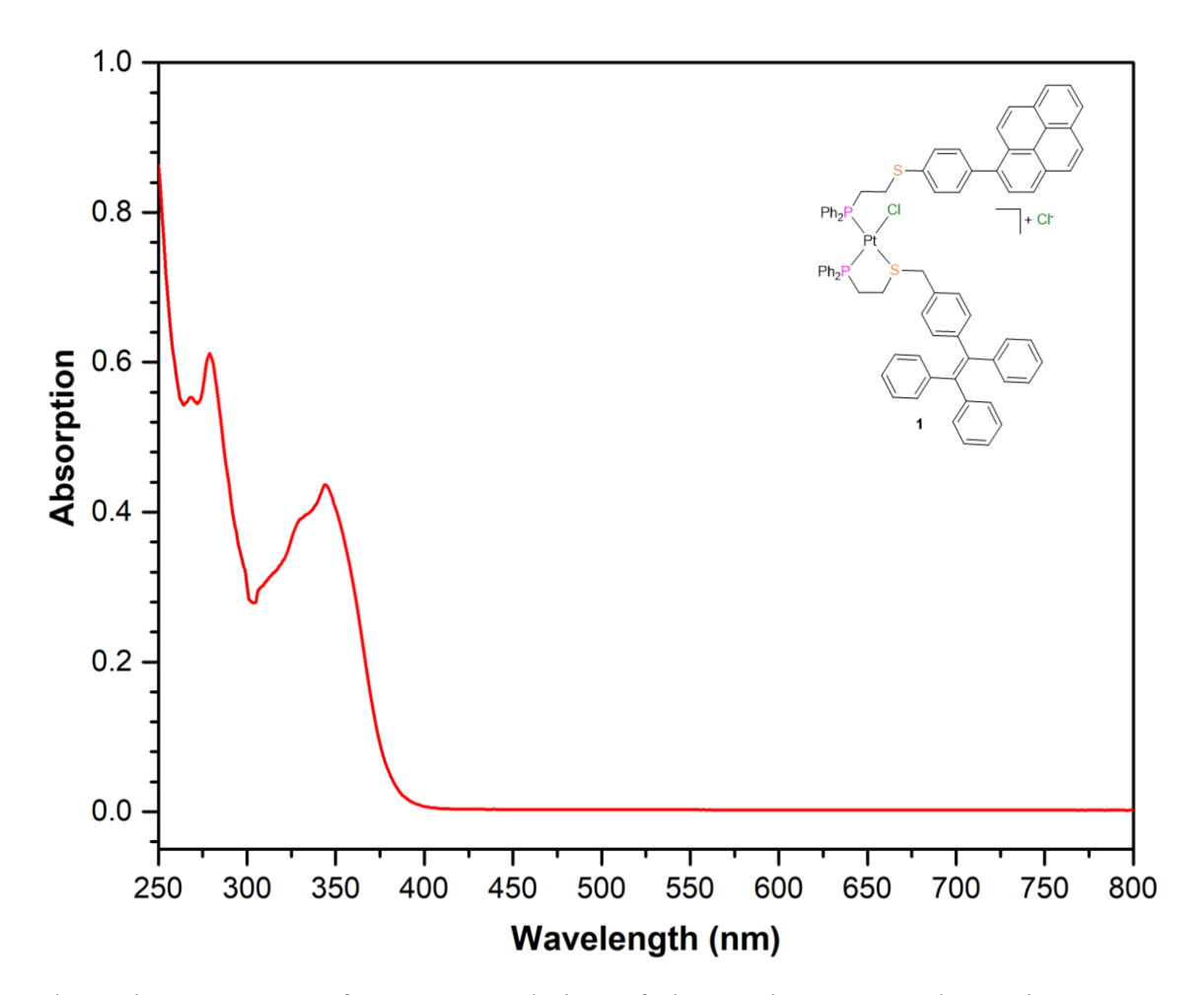


Fig. S2. Formation of aggregates resulted in enhanced fluorescence emission. Photographs of the solutions or suspensions of (a) 1 and (b) 2 in DCM/hexane mixtures with different volumetric fractions of hexane. Stacked fluorescence emission spectra of the solutions or suspensions of (c) 1 and (d) 2 in DCM/hexane mixtures. Concentration: 1 (0.4 mM); 2 (0.5 mM). Excitation wavelength: 344 nm.

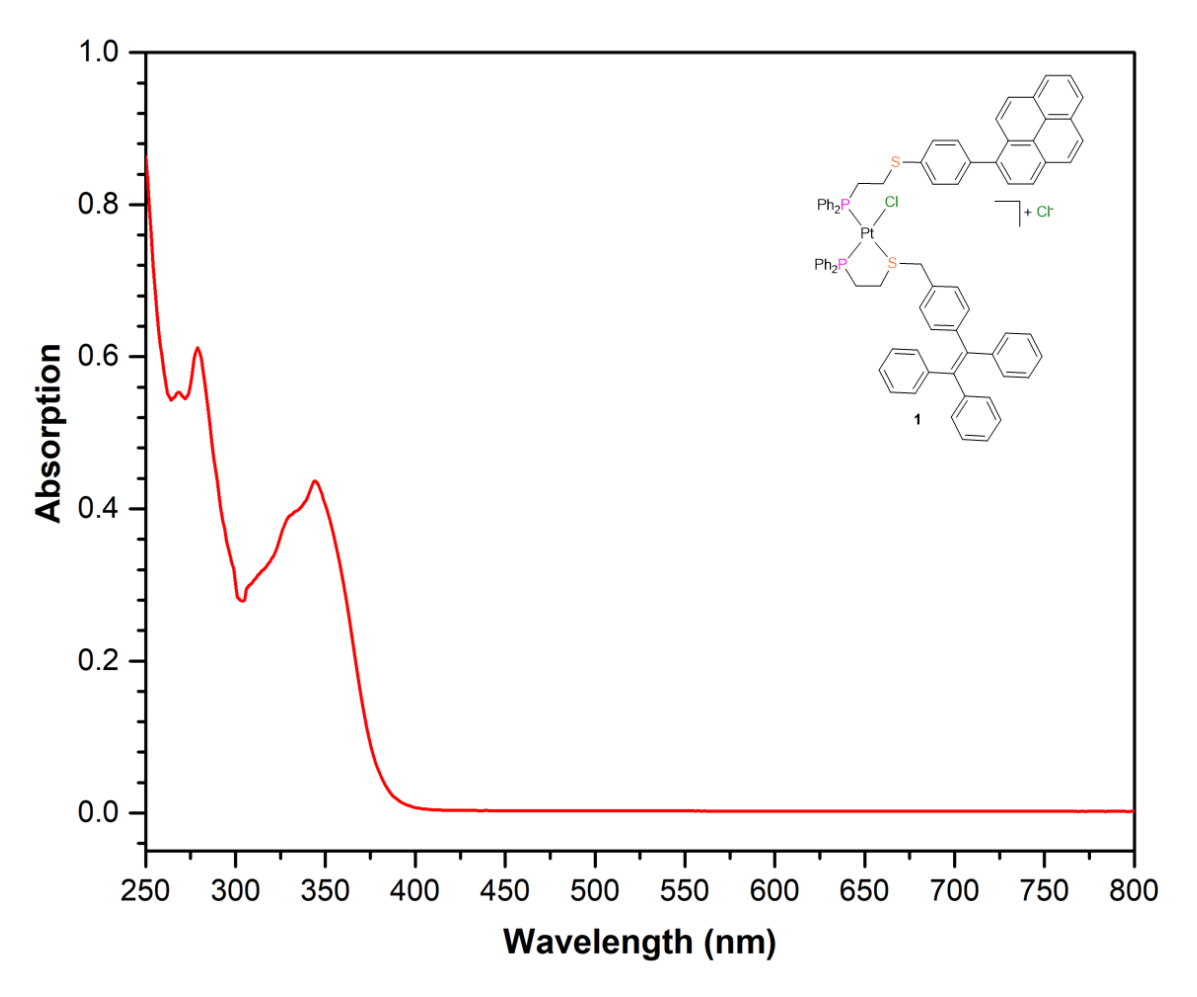
Absorption Spectra



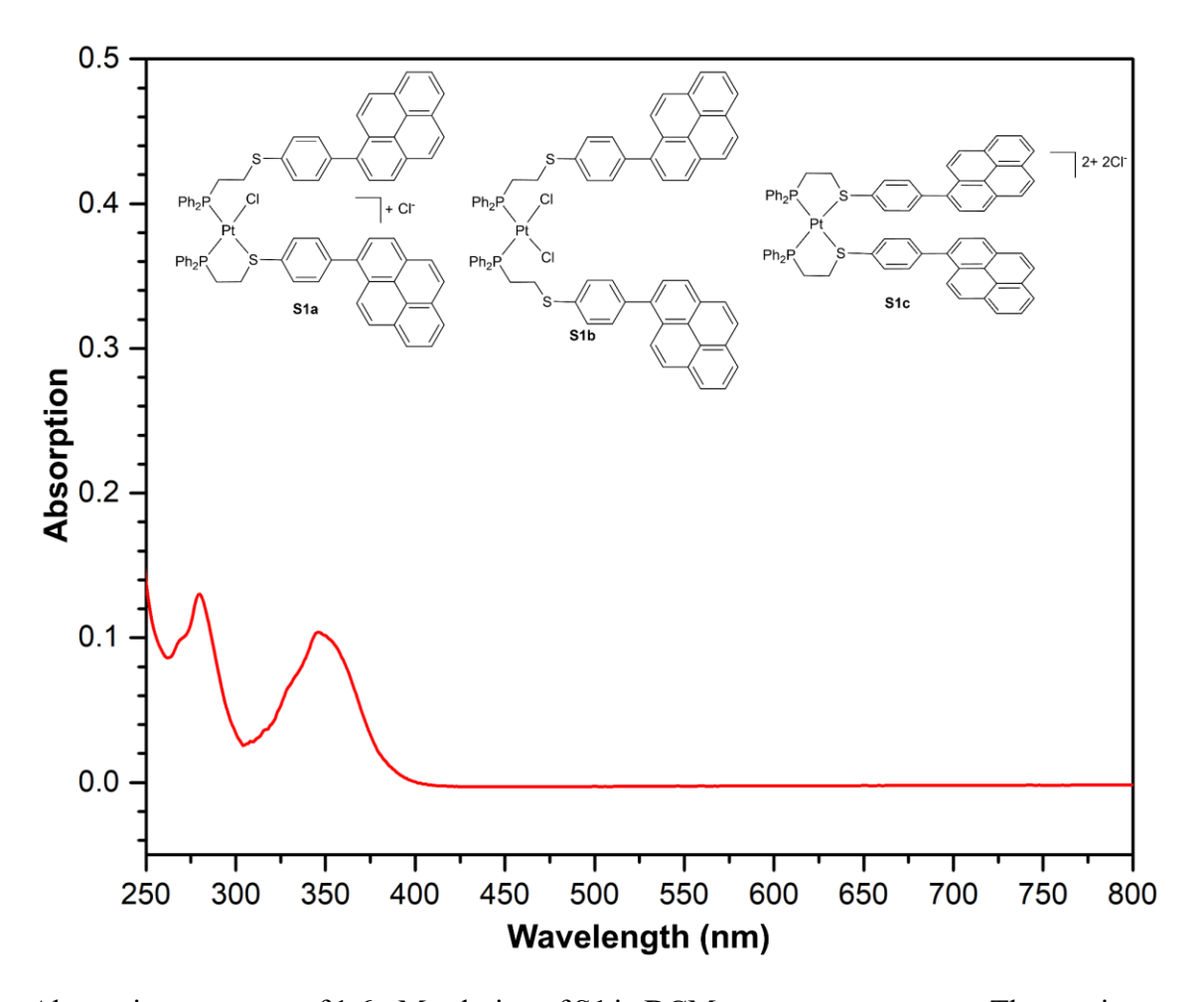
Absorption spectra of 1 (16.8 μ M), 2 (8.8 μ M), S1 (1.6 μ M), S2 (1.4 μ M), and S3 (2.7 μ M) in DCM at room temperature.



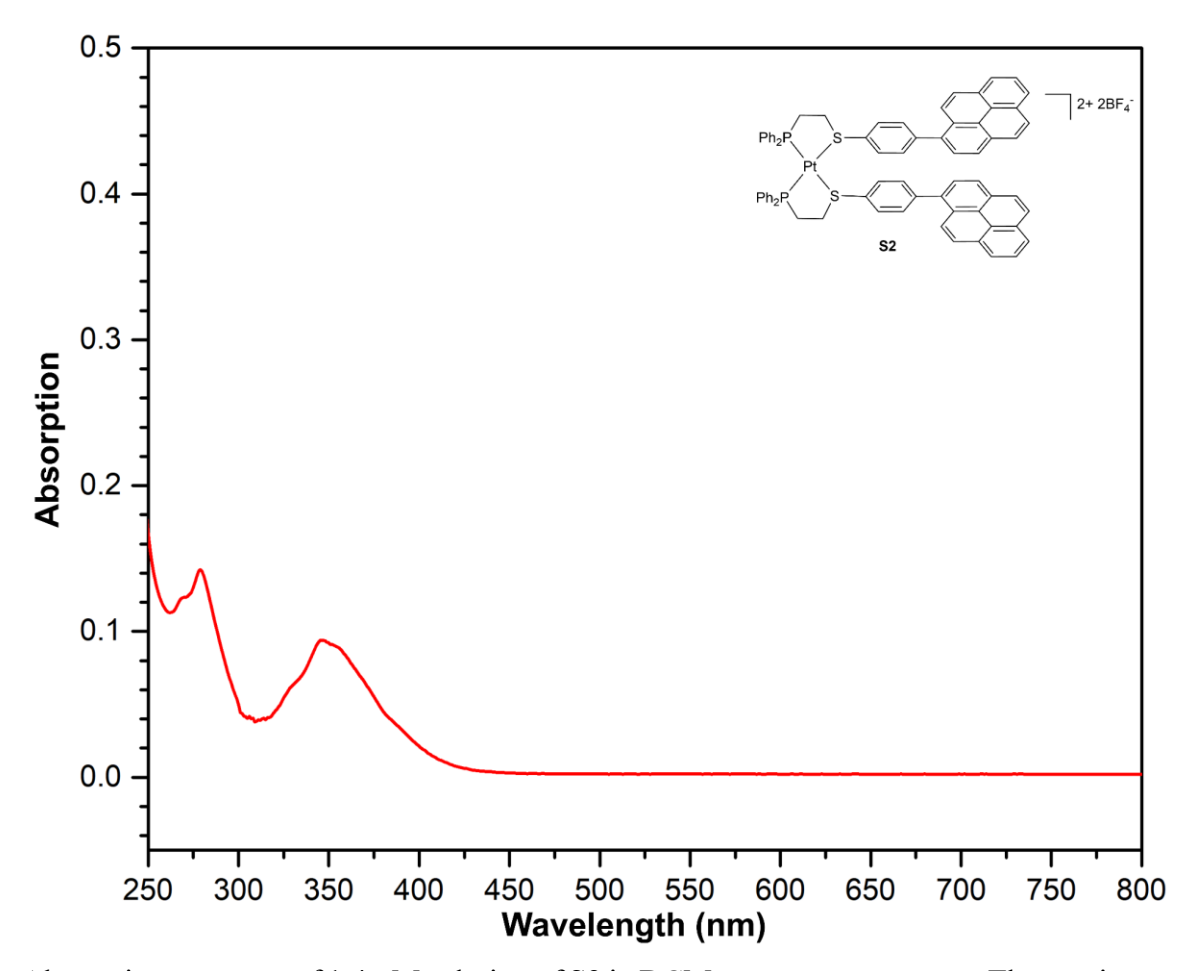
Absorption spectrum of 16.8 μ M solution of the semi-open complex 1 in DCM at room temperature. The maximum λ_{abs} : 344 nm. Calculated molar absorptivity constant for 1: ϵ = 2.6E4 $M^{-1} \cdot cm^{-1}$.



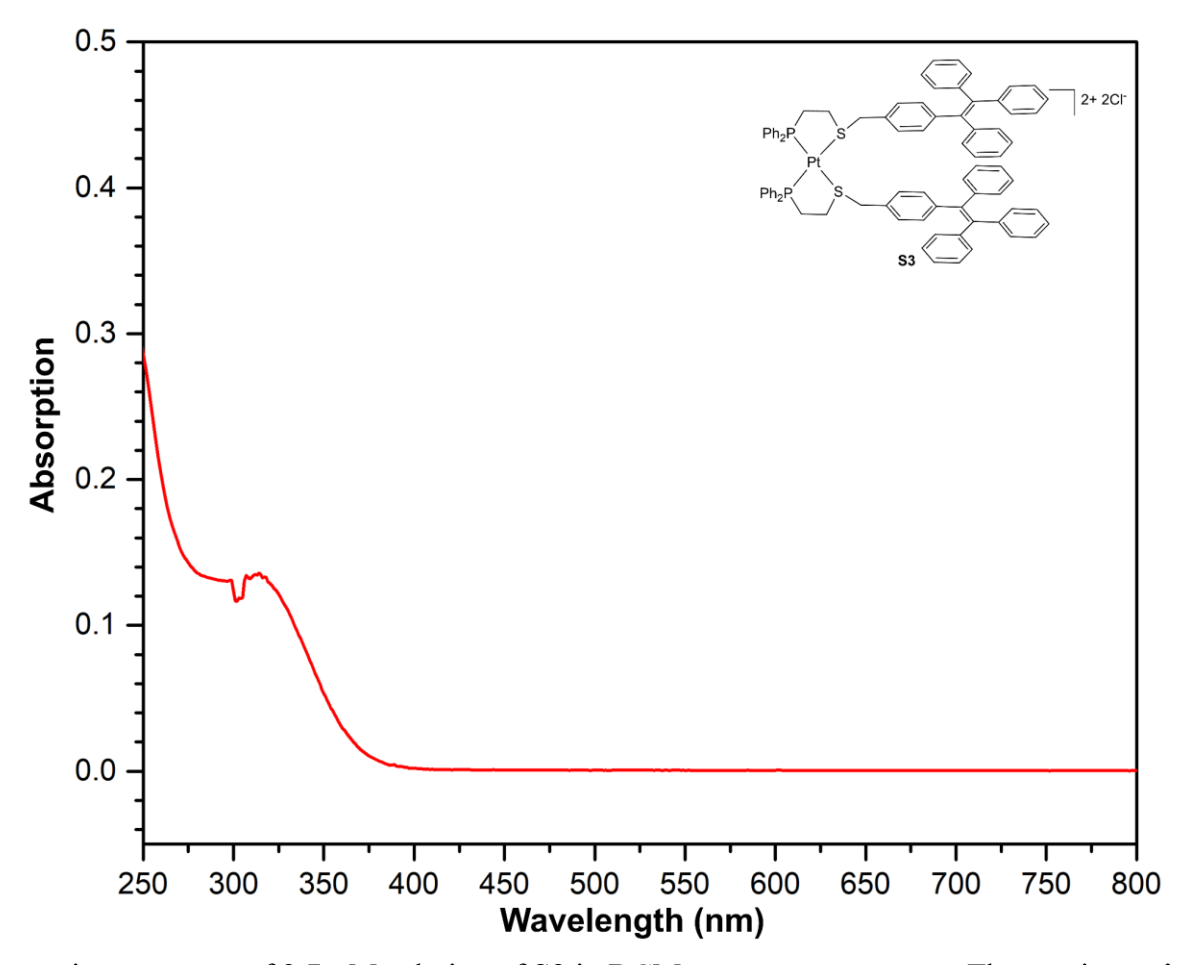
Absorption spectrum of 8.8 μM solution of the closed complex 2 in DCM at room temperature. The maximum λ_{abs} : 344 nm. Calculated molar absorptivity constant for 2: $\epsilon = 2.14 E4 \ M^{-1} \cdot cm^{-1}$.



Absorption spectrum of 1.6 μM solution of S1 in DCM at room temperature. The maximum λ_{abs} : 344 nm.

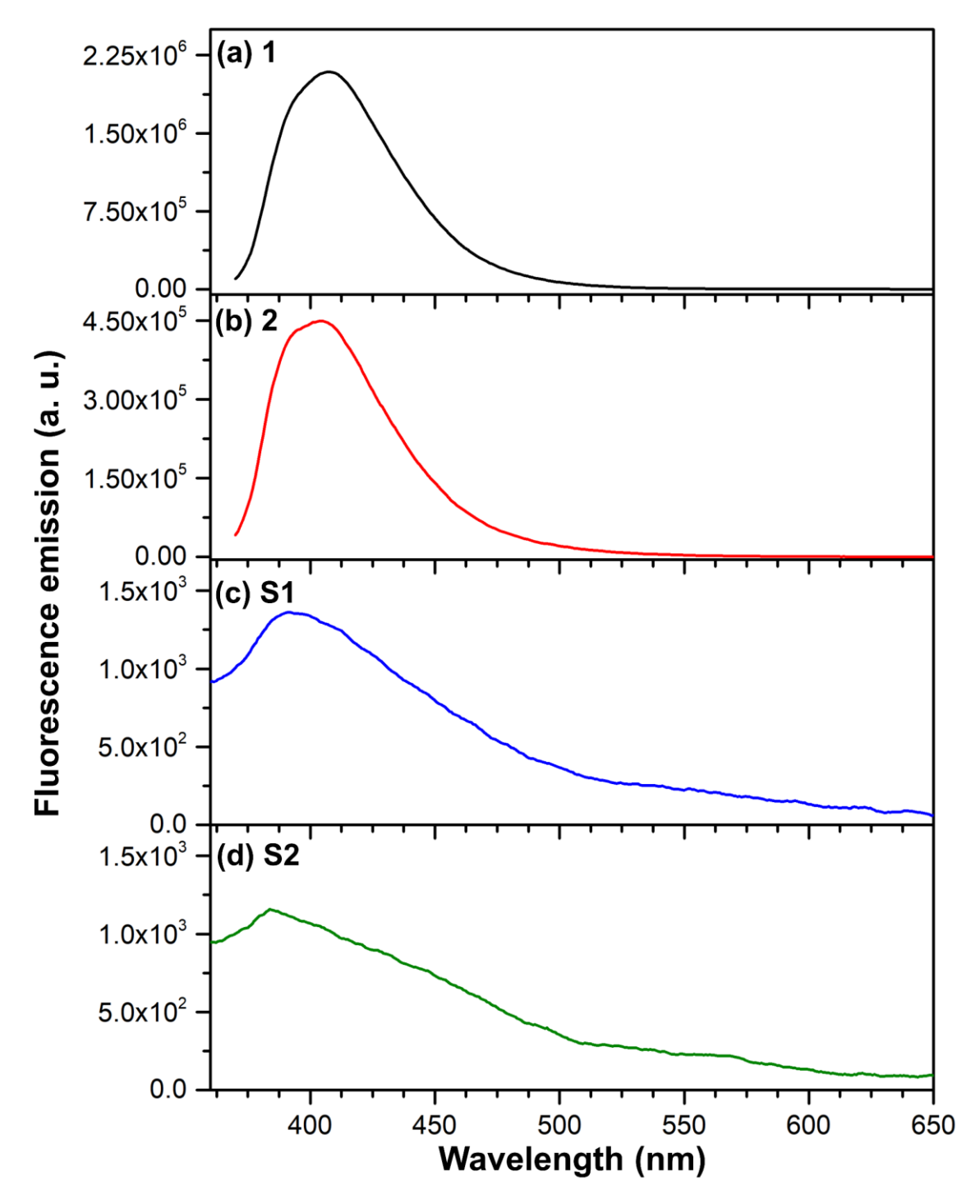


Absorption spectrum of 1.4 μM solution of S2 in DCM at room temperature. The maximum $\lambda_{abs}\!\!:$ 344 nm.

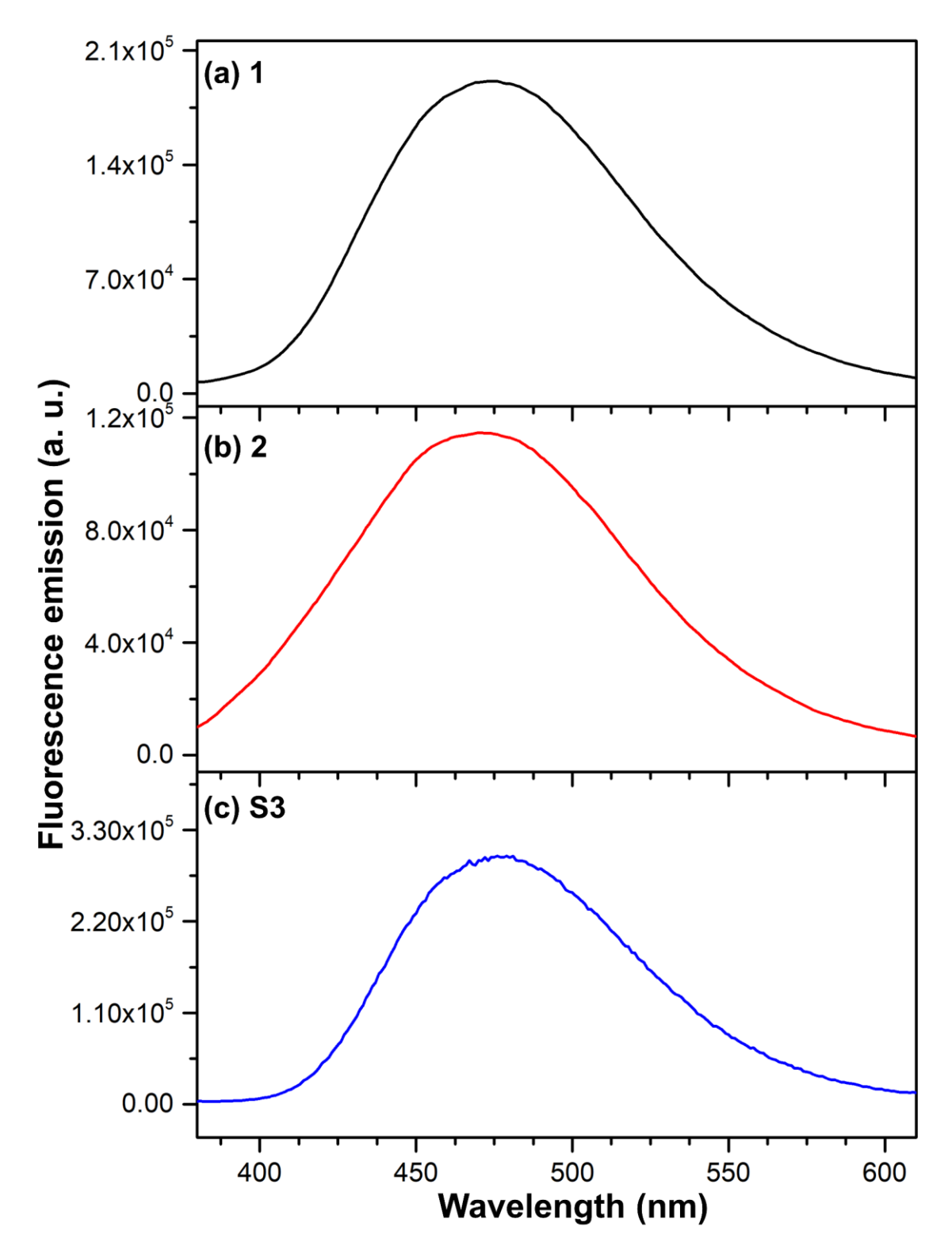


Absorption spectrum of 2.7 μM solution of S3 in DCM at room temperature. The maximum λ_{abs} : 311 nm.

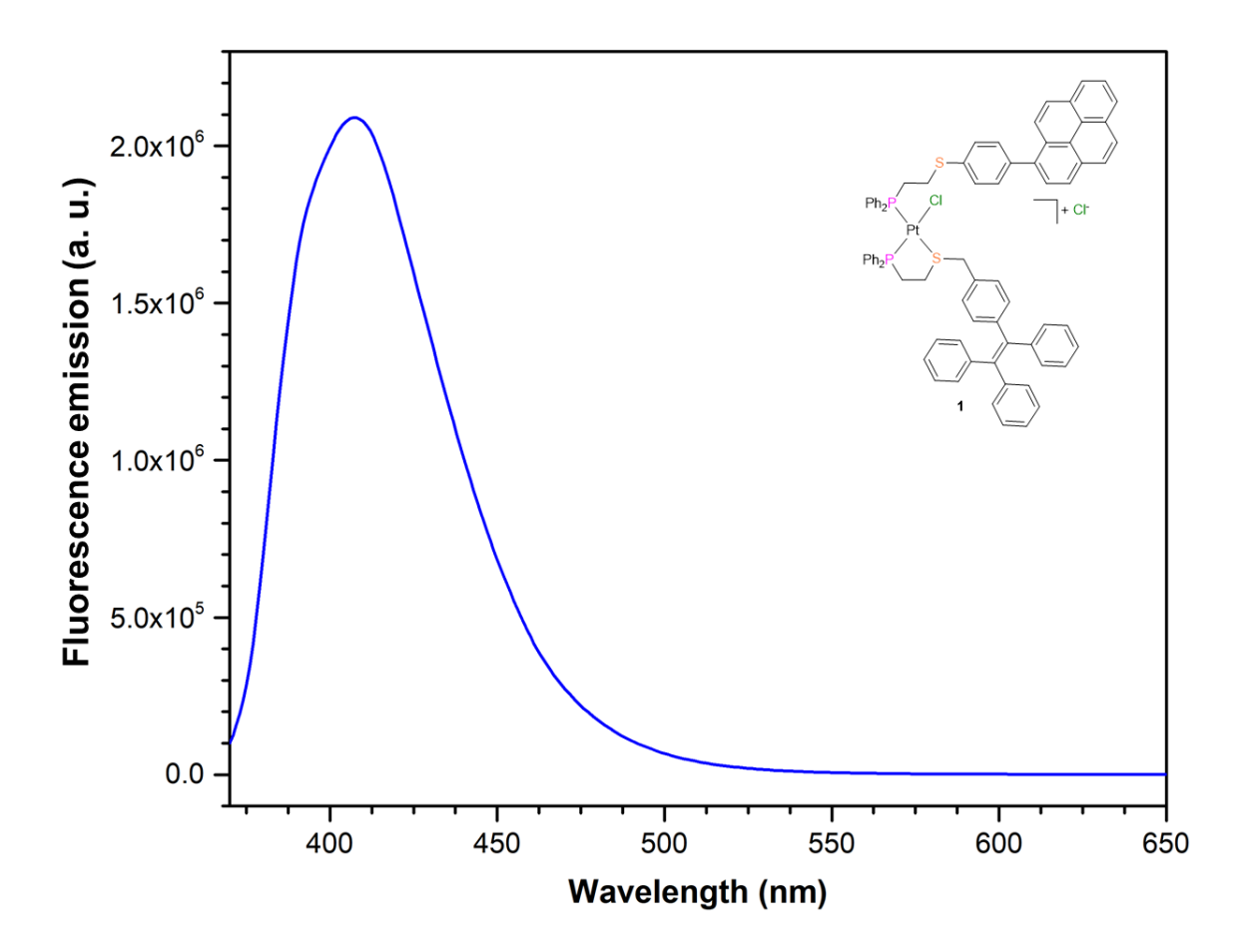
Fluorescence Spectra



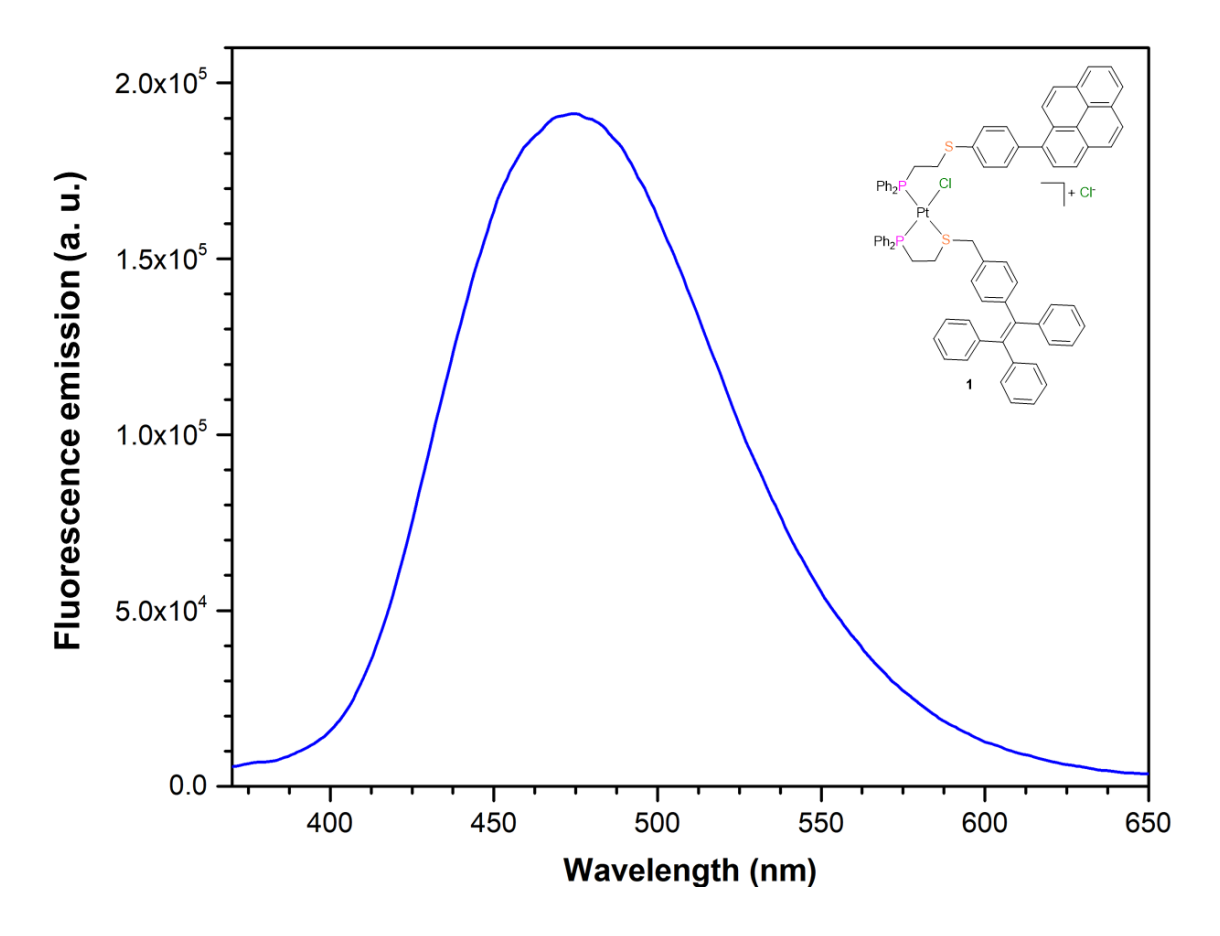
Fluorescence emission spectra of (a) a DCM solution of 1 (3.4 μ M). The maximum λ_{em} : 407 nm; (b) a DCM solution of 2 (3.5 μ M). The maximum λ_{em} : 404 nm; (c) a DCM solution of S1 (1.6 μ M). The maximum λ_{em} : 391 nm; (d) a DCM solution of S2 (1.4 μ M). The maximum λ_{em} : 386 nm. Excitation wavelength: 344 nm.



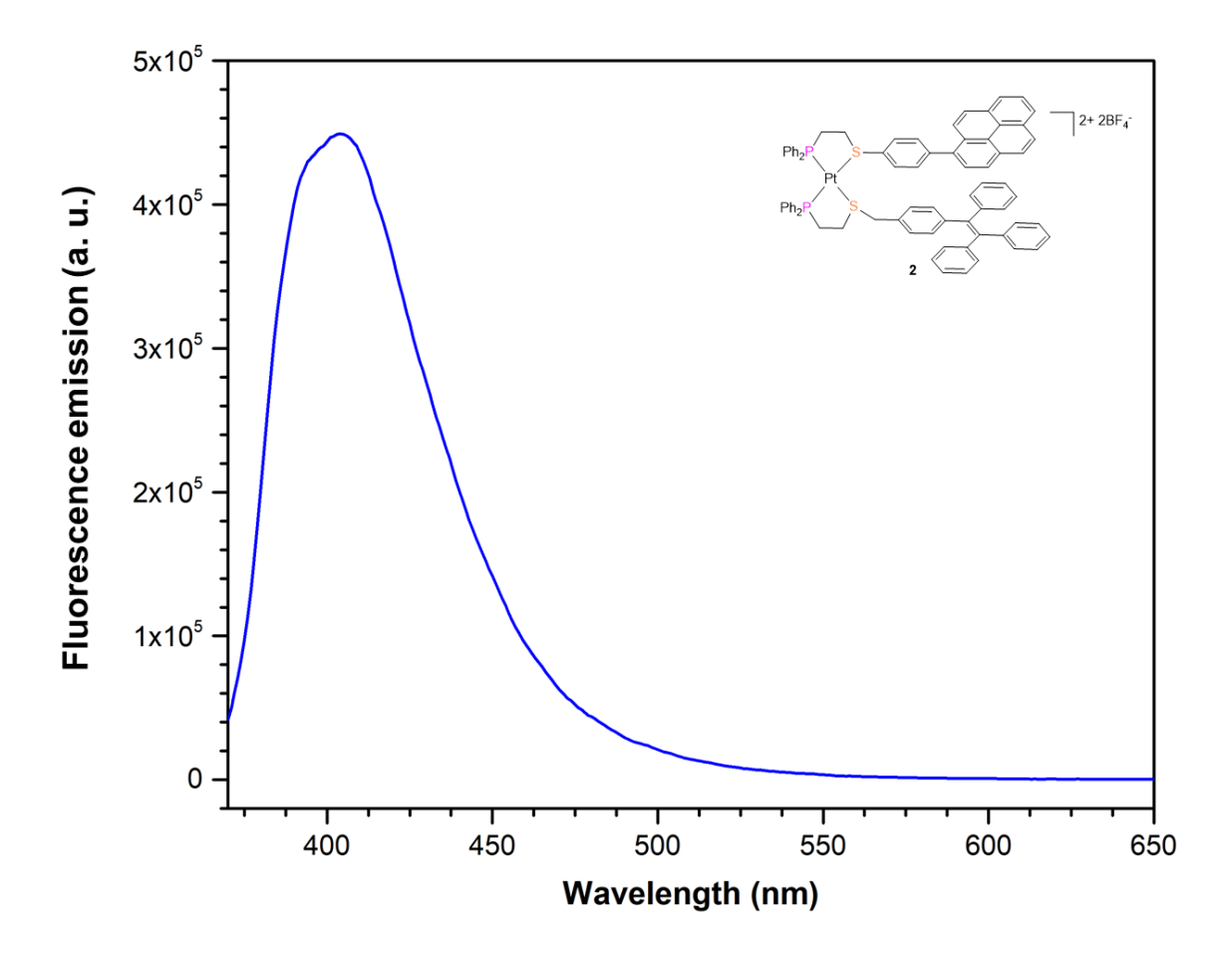
Fluorescence emission spectra of (a) solid-state 1 drop-casted on powder cups. The maximum λ_{em} : 475 nm; (b) solid-state 2 drop-casted on powder cups. The maximum λ_{em} : 470 nm; (c) solid-state S3 drop-casted on powder cups. The maximum λ_{em} : 481 nm. Excitation wavelength: 344 nm for 1 and 2; 311 nm for S3.



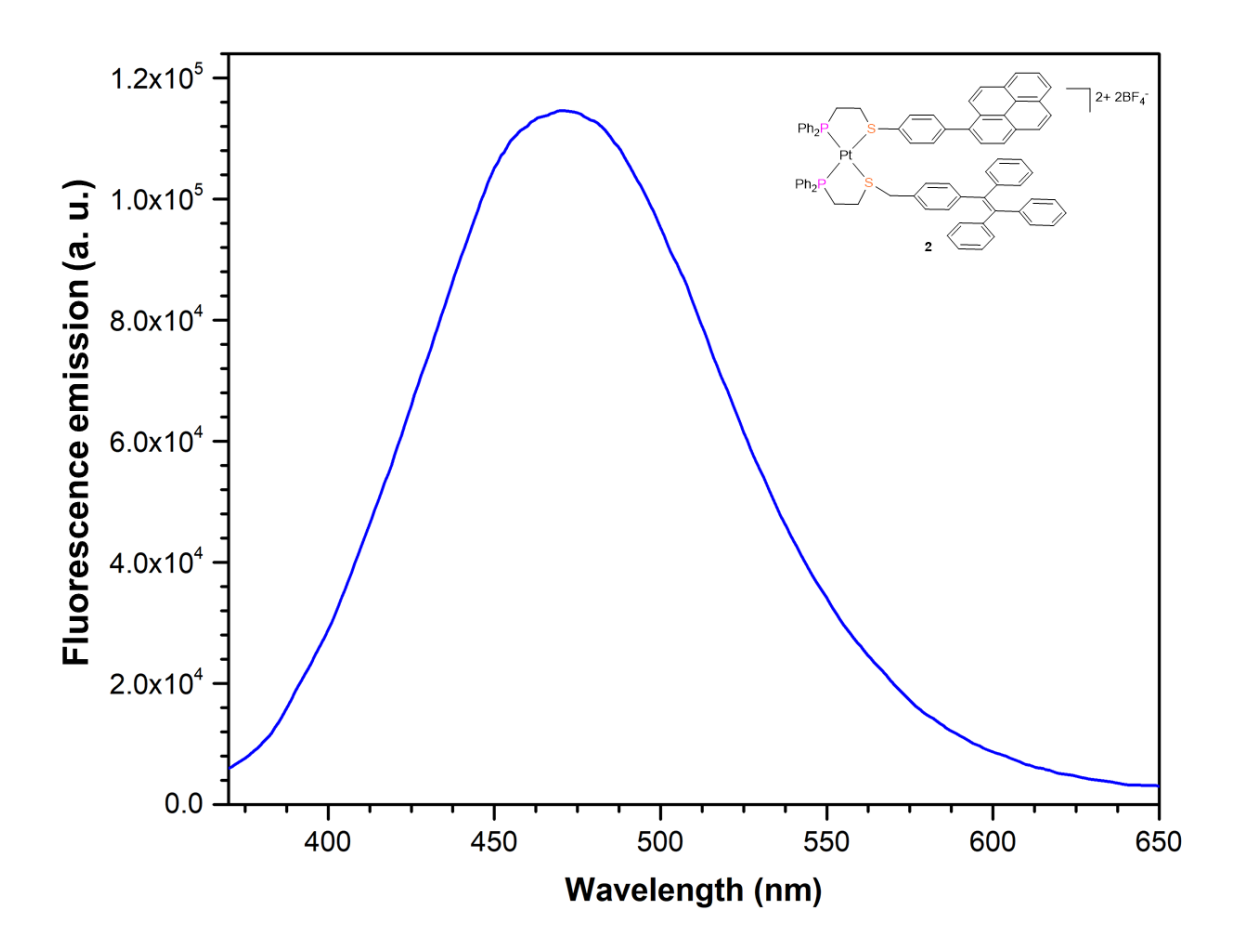
Fluorescence emission spectrum of a DCM solution of semi-open complex 1 (3.4 μ M). The maximum λ_{em} : 407 nm. Excitation wavelength: 344 nm.



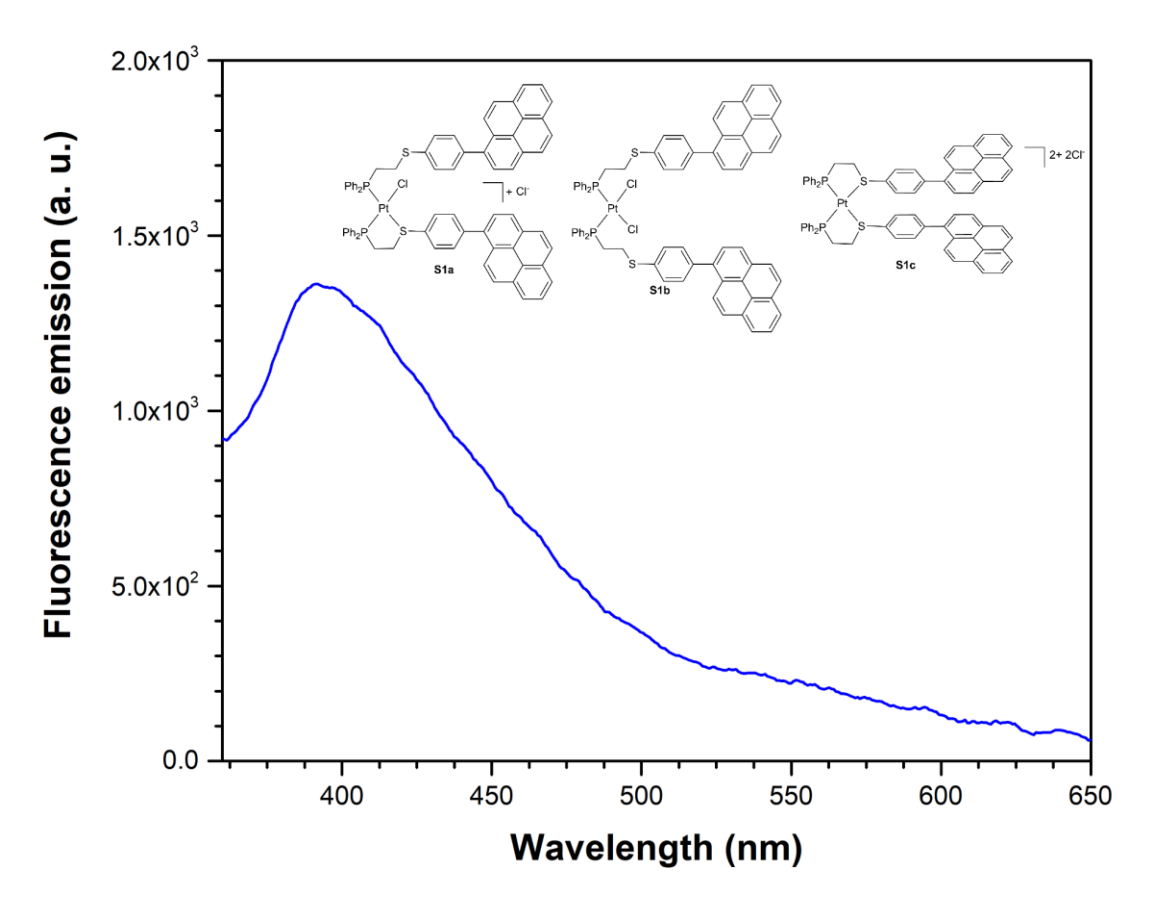
Fluorescence emission spectrum of solid-state semi-open complex 1 drop-casted on powder cups. The maximum λ_{em} : 475 nm. Excitation wavelength: 344 nm.



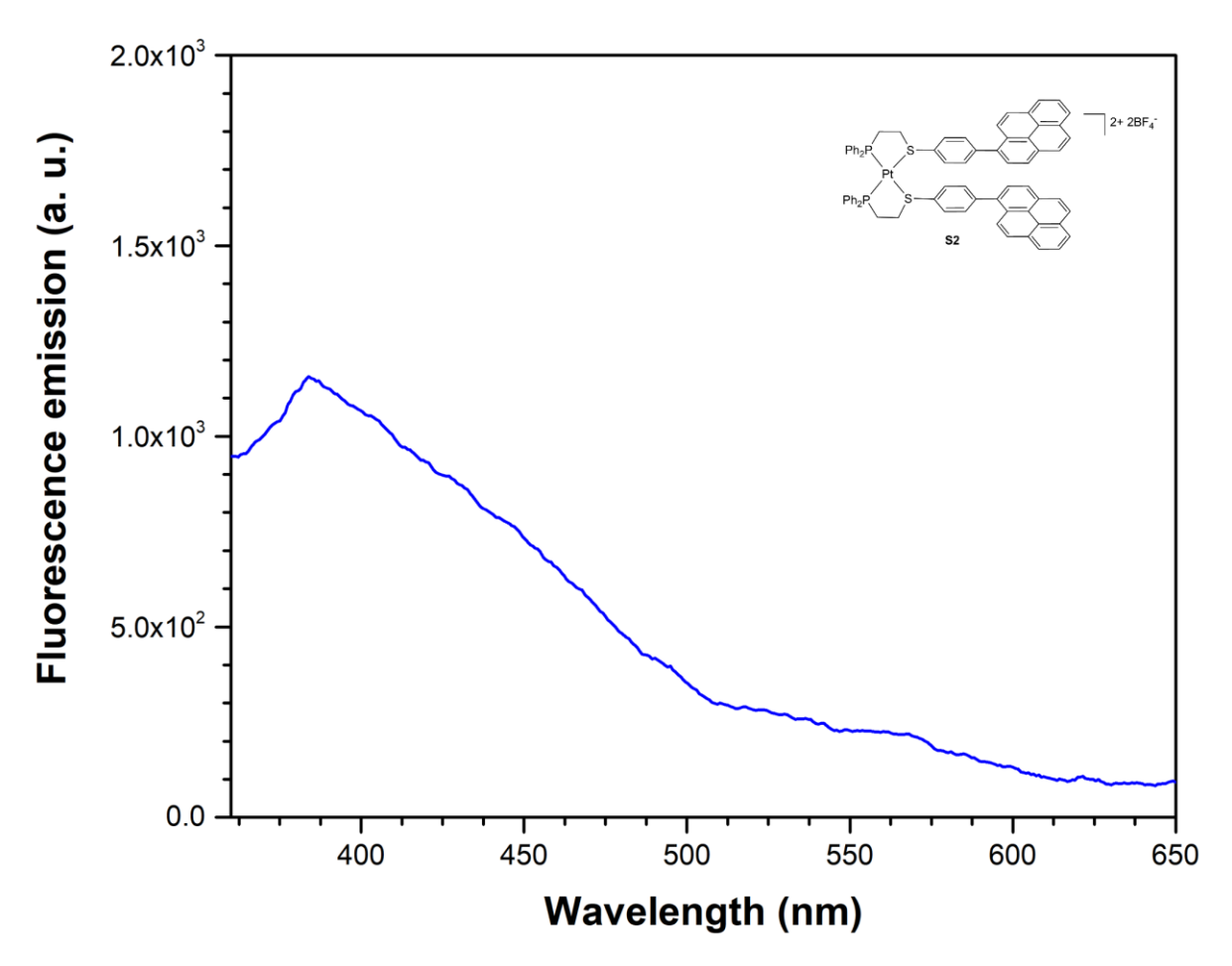
Fluorescence emission spectrum of a DCM solution of closed complex 2 (3.5 μ M). The maximum λ_{em} : 404 nm. Excitation wavelength: 344 nm.



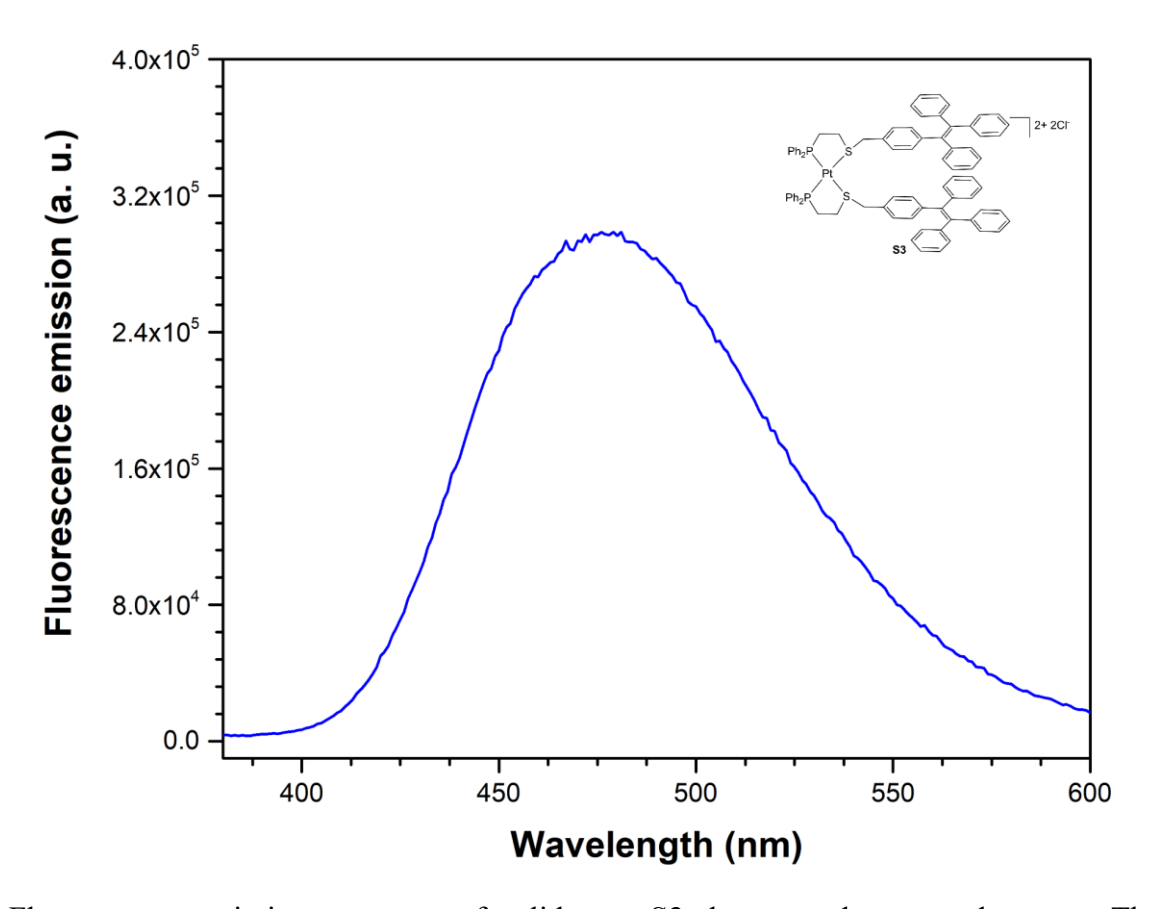
Fluorescence emission spectrum of solid-state closed complex ${\bf 2}$ drop-casted on powder cups. The maximum λ_{em} : 470 nm. Excitation wavelength: 344 nm.



Fluorescence emission spectrum of a DCM solution of S1 (1.6 μ M). The maximum λ_{em} : 391 nm. Excitation wavelength: 344 nm.

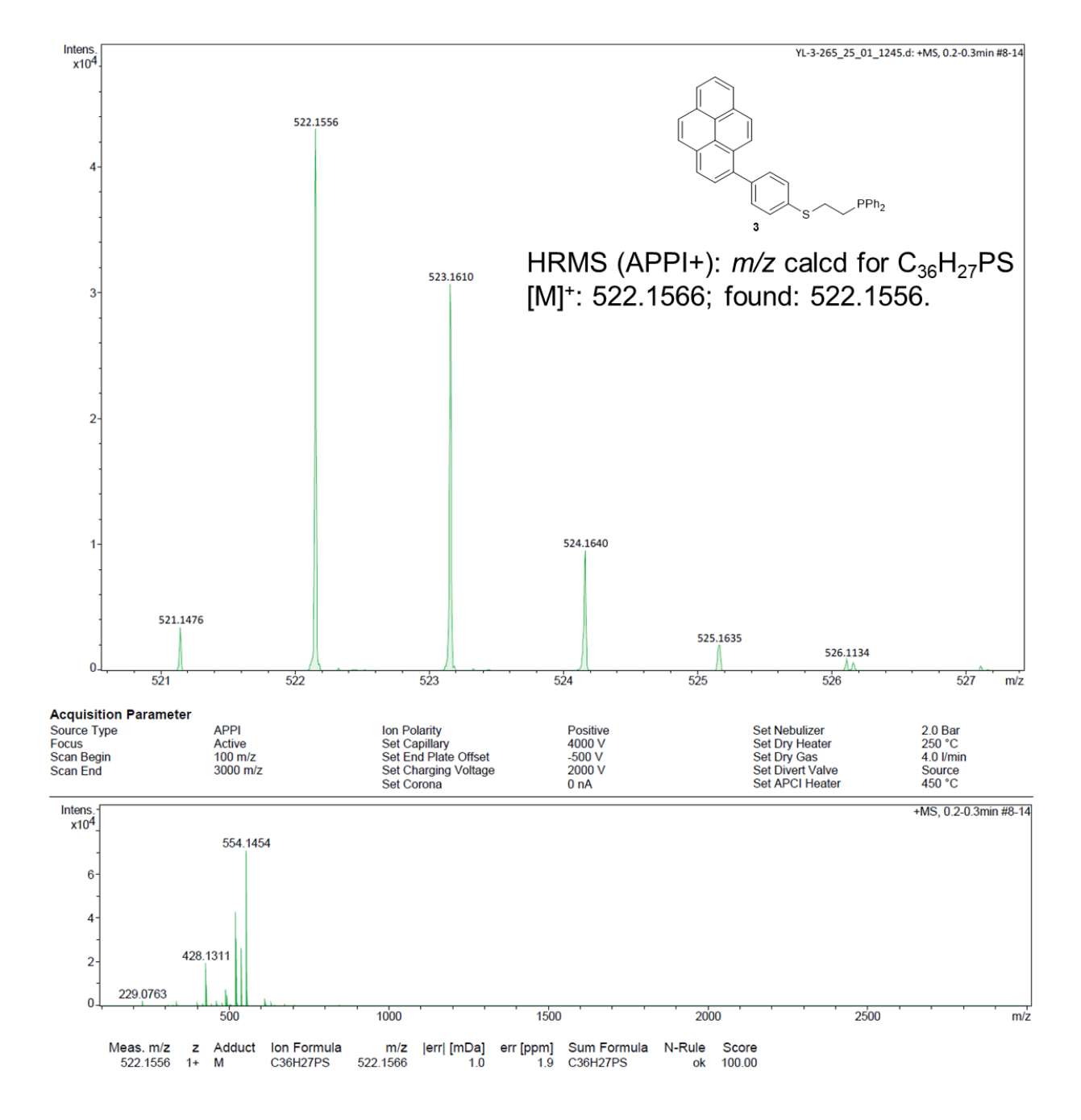


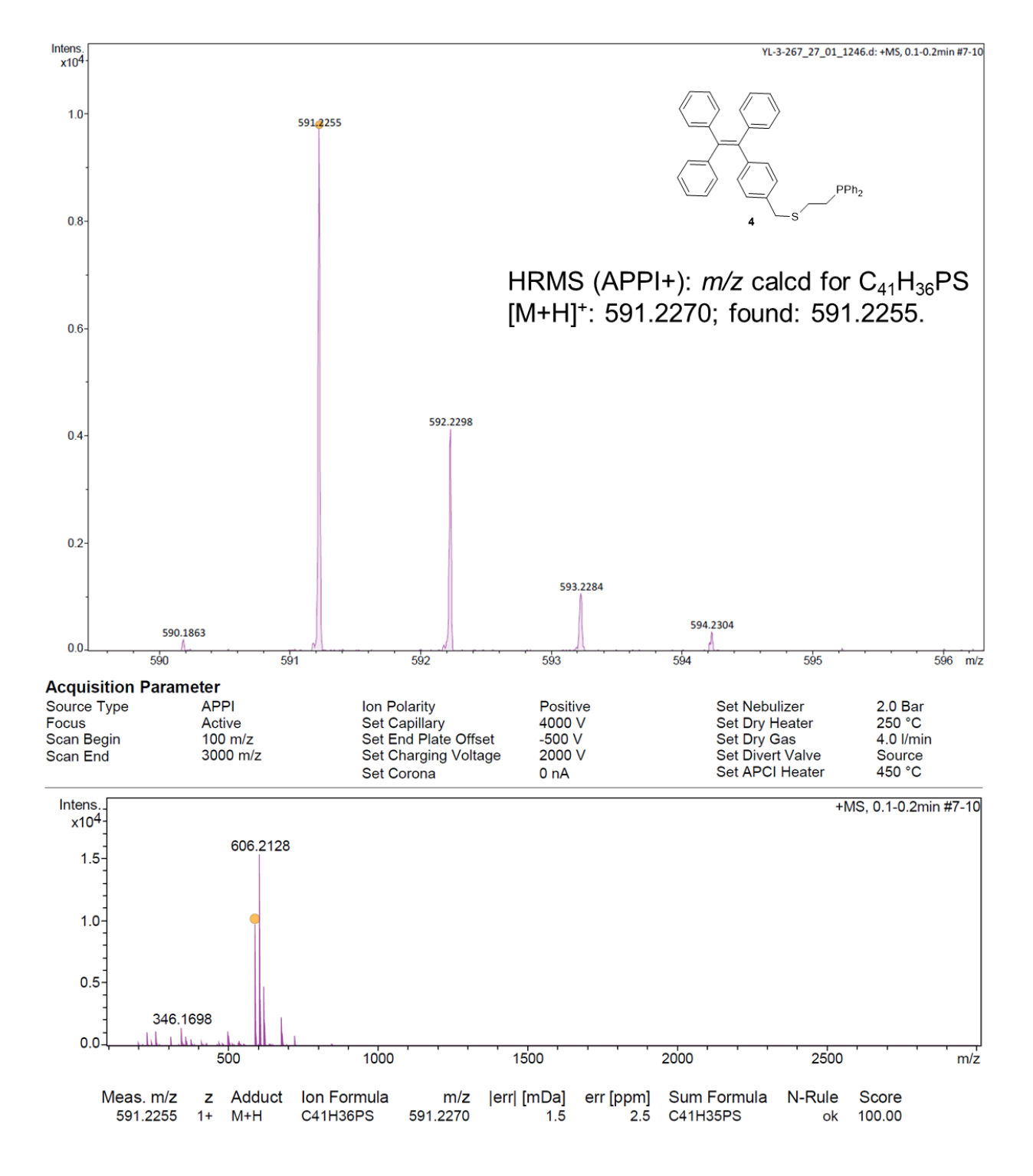
Fluorescence emission spectrum of a DCM solution of S2 (1.4 μ M). The maximum λ_{em} : 386 nm. Excitation wavelength: 344 nm.

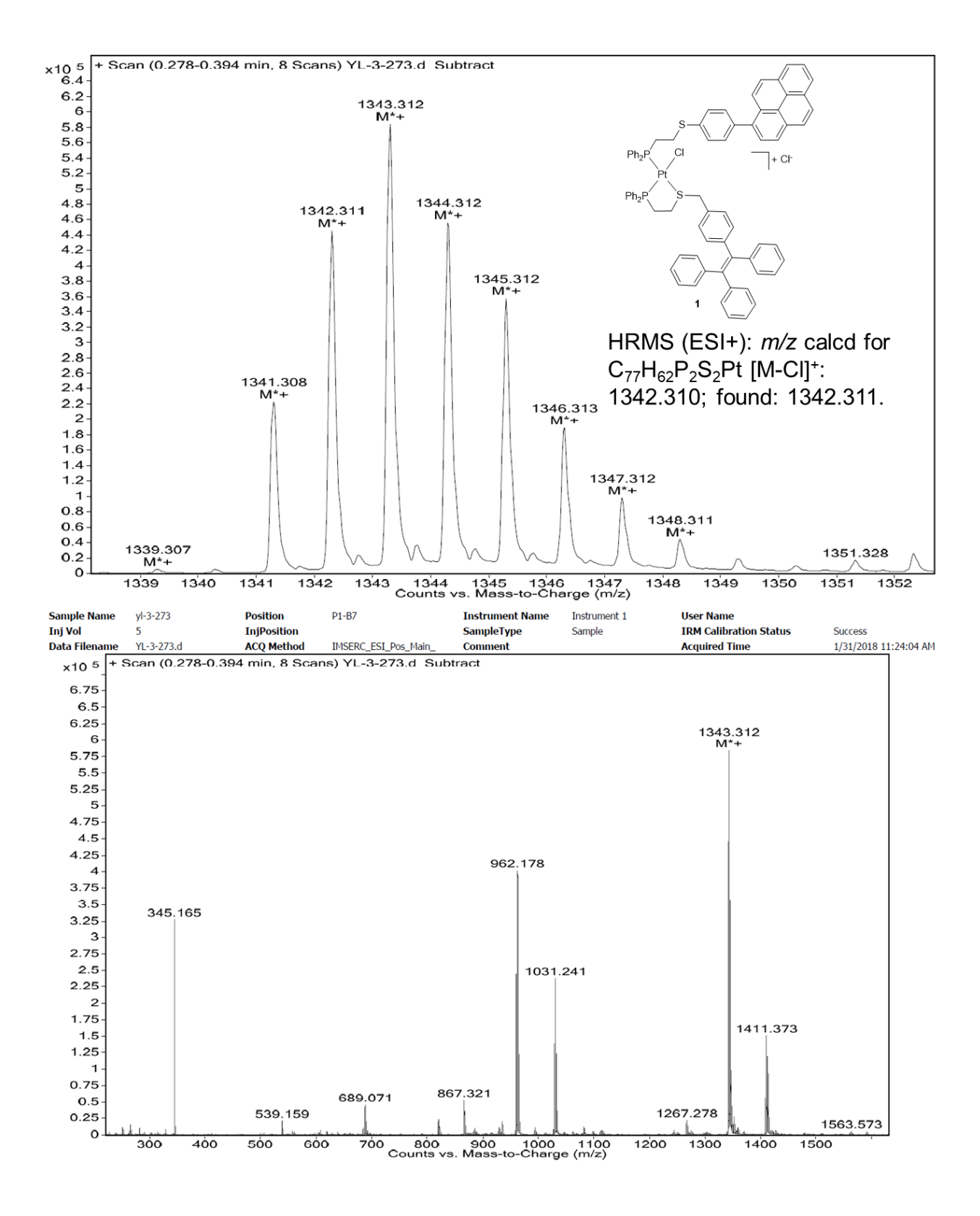


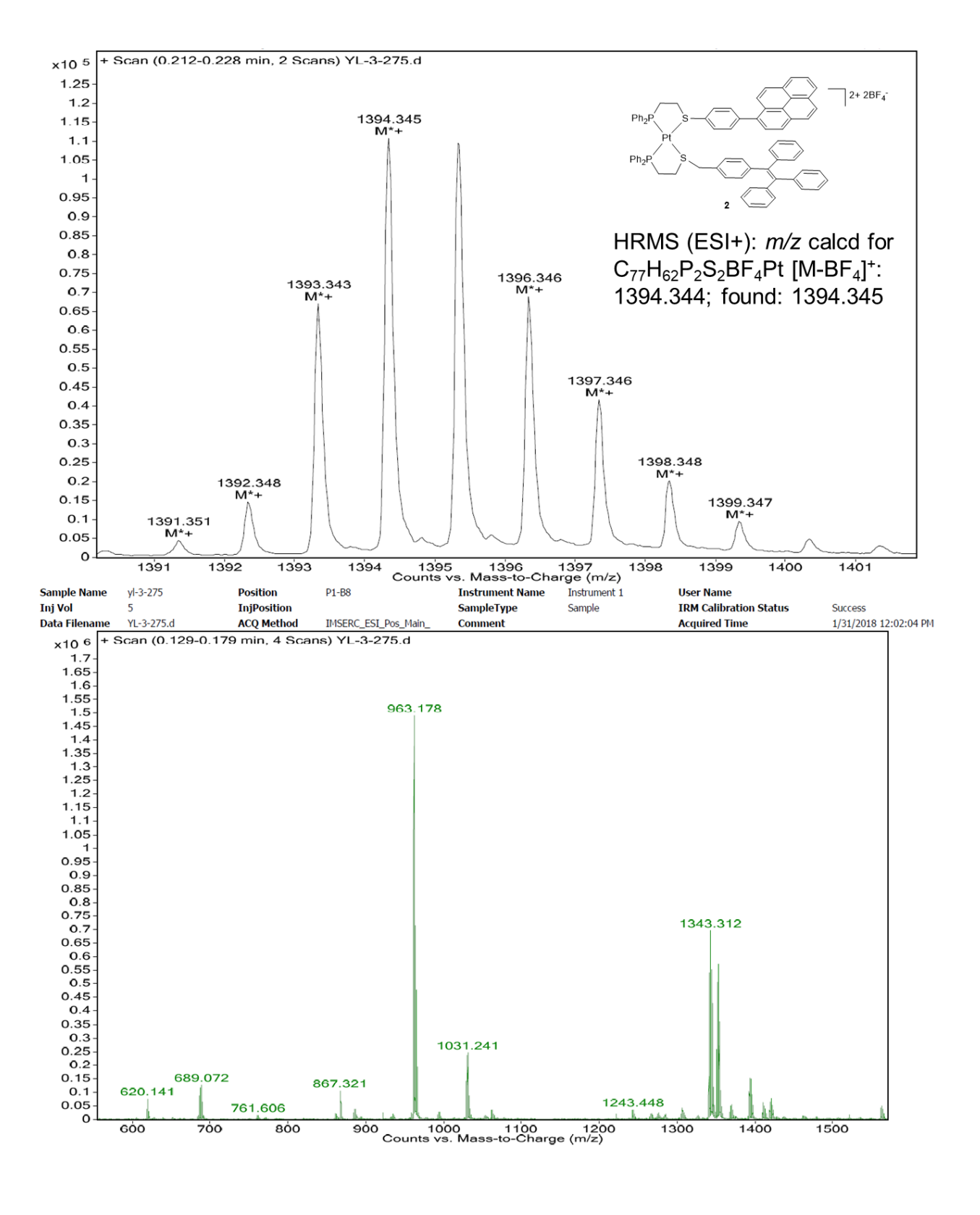
Fluorescence emission spectrum of solid-state S3 drop-casted on powder cups. The maximum λ_{em} : 481 nm. Excitation wavelength: 311 nm.

High Resolution Mass Spectra

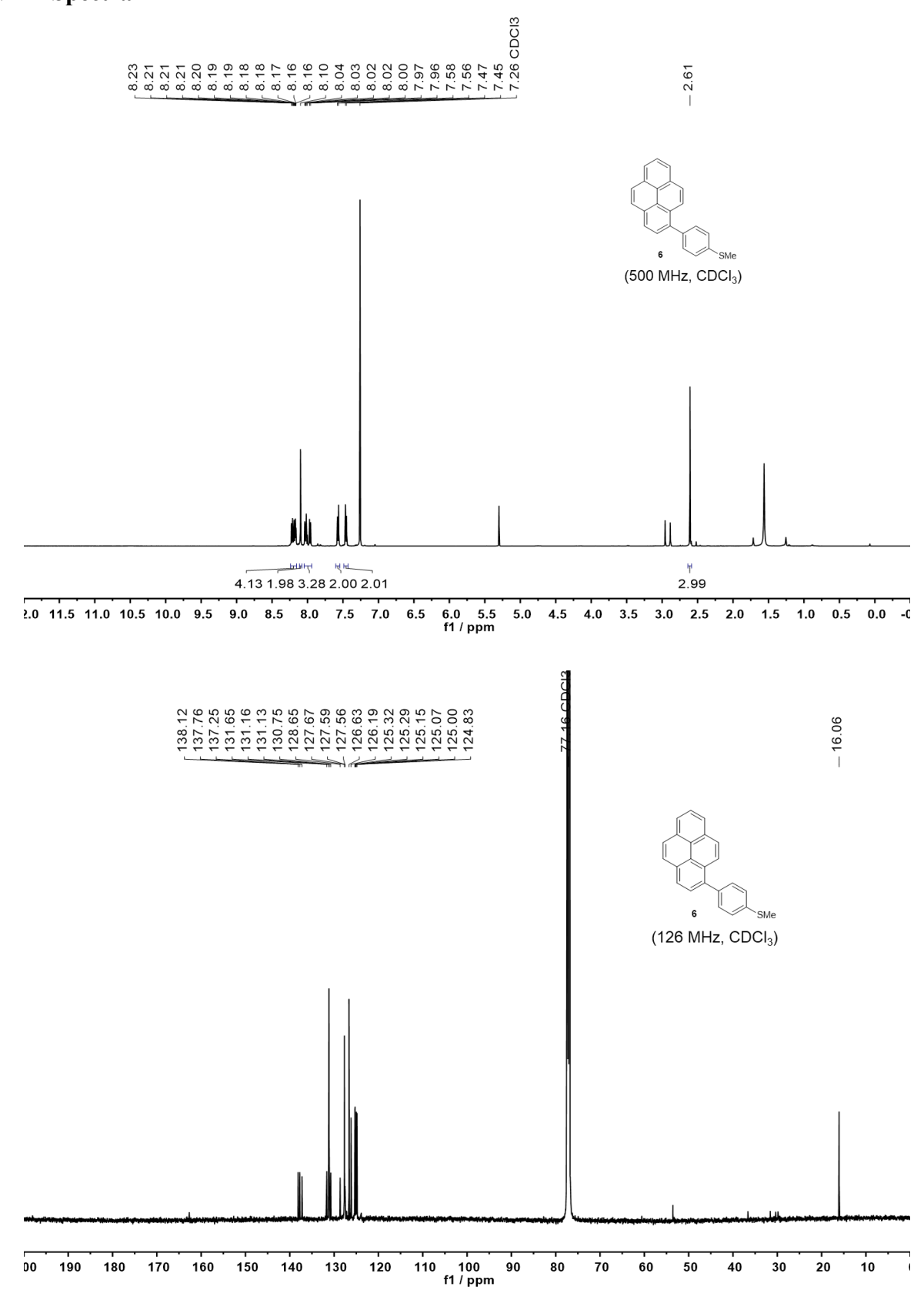


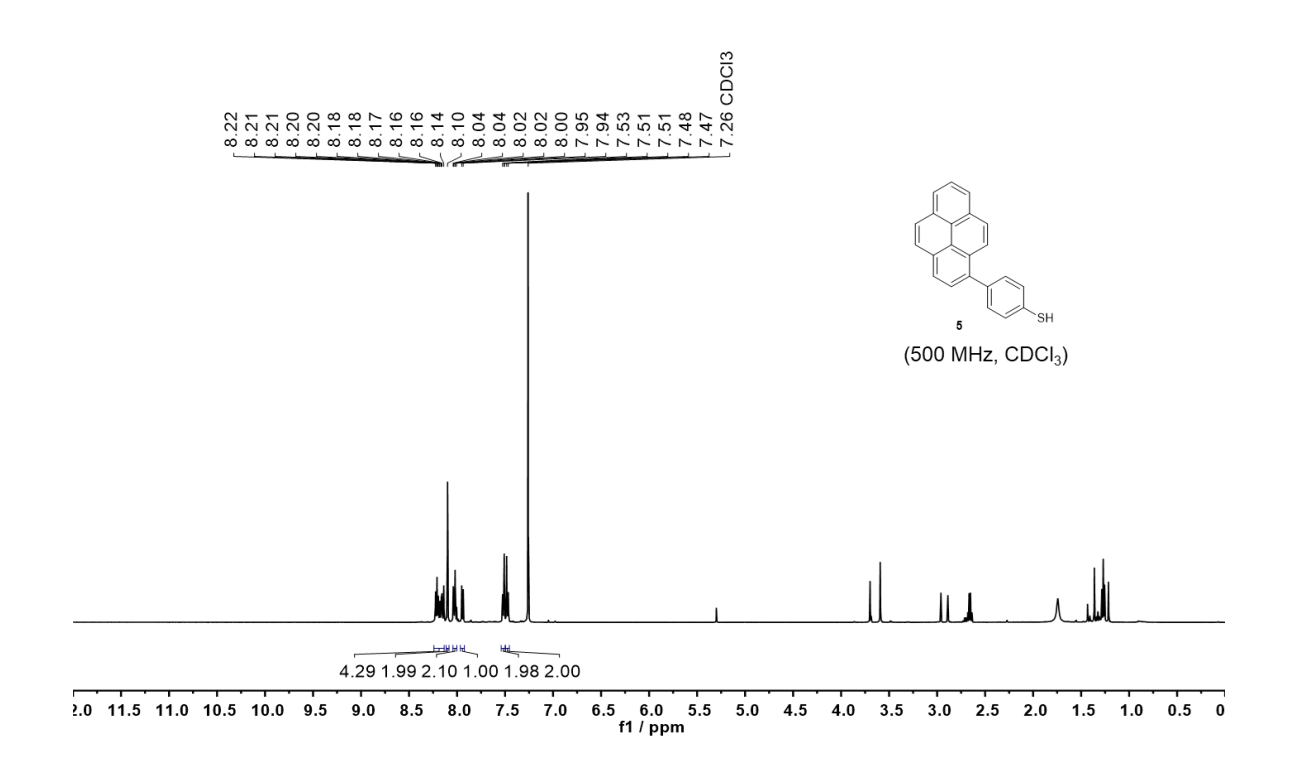


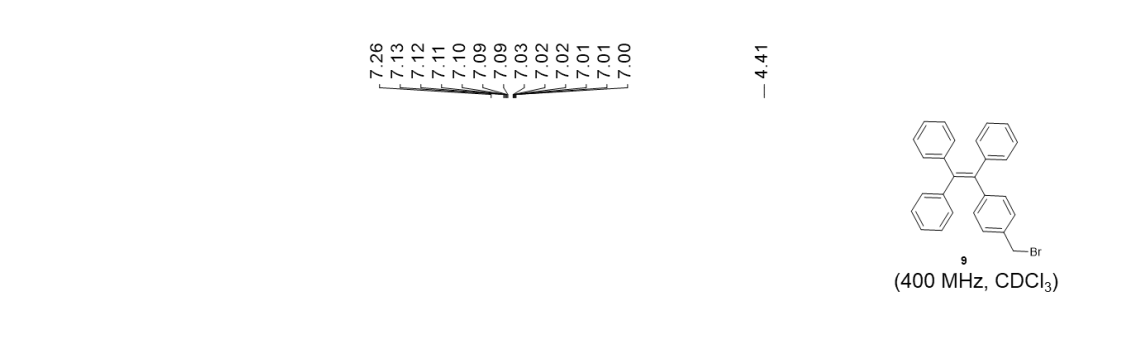


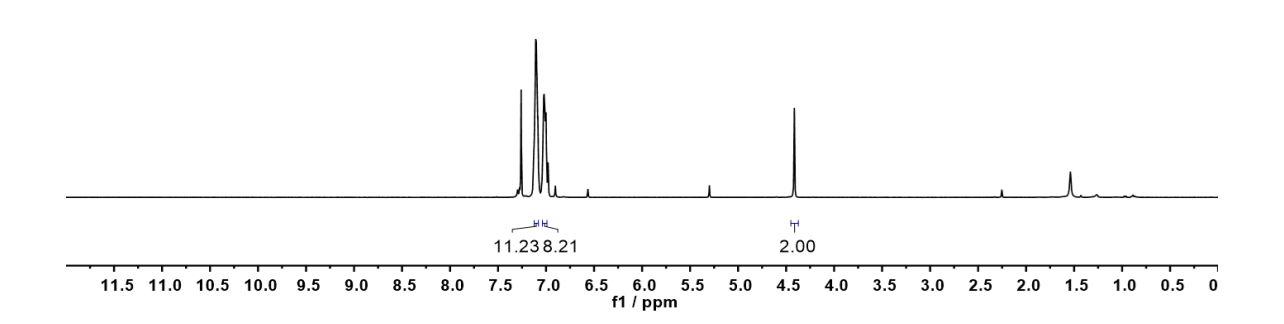


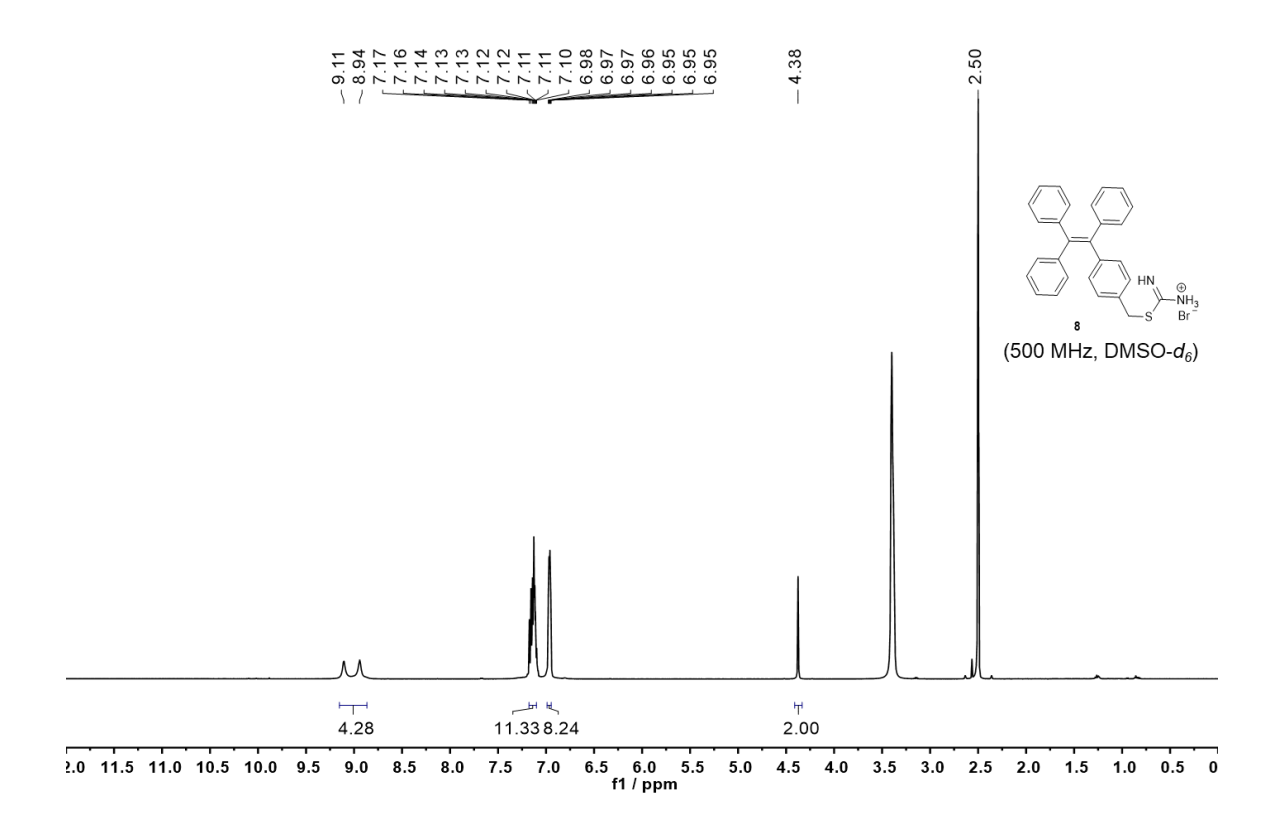
NMR Spectra

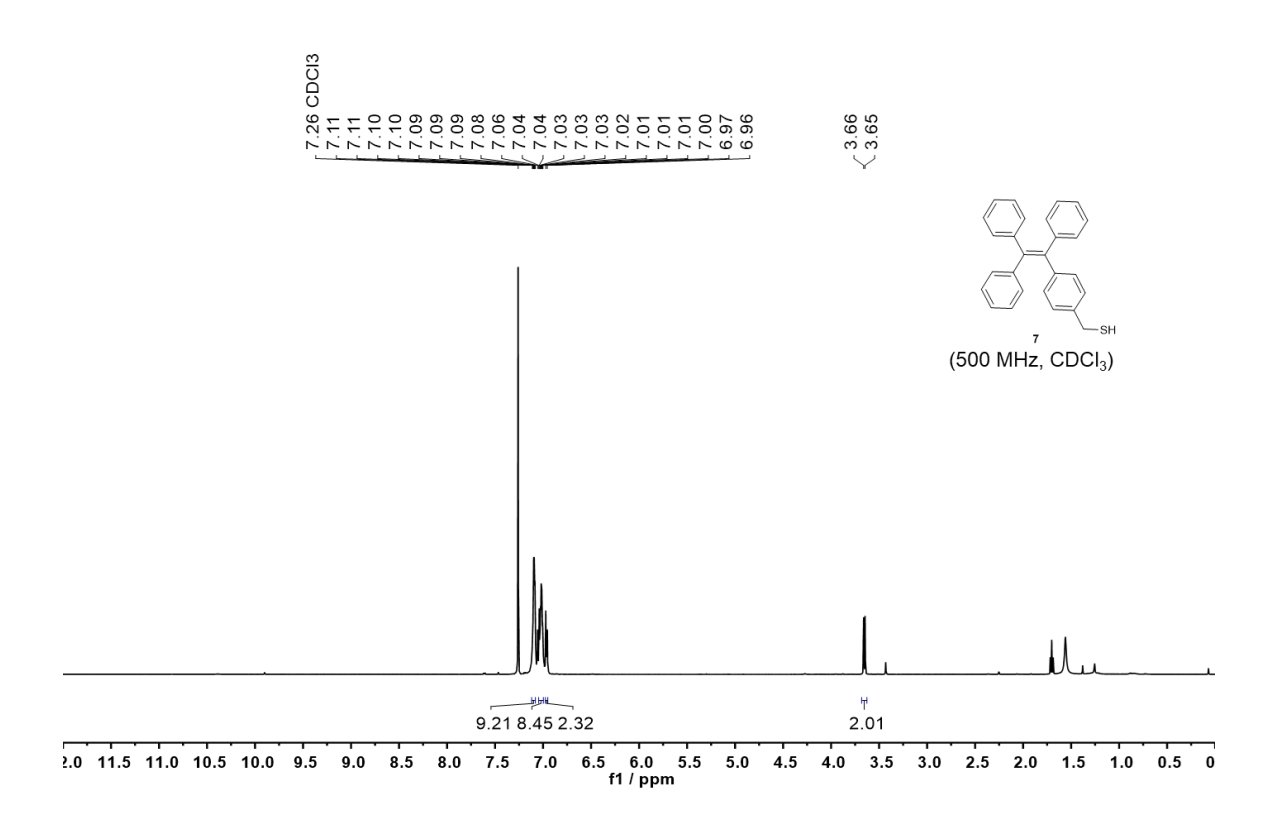


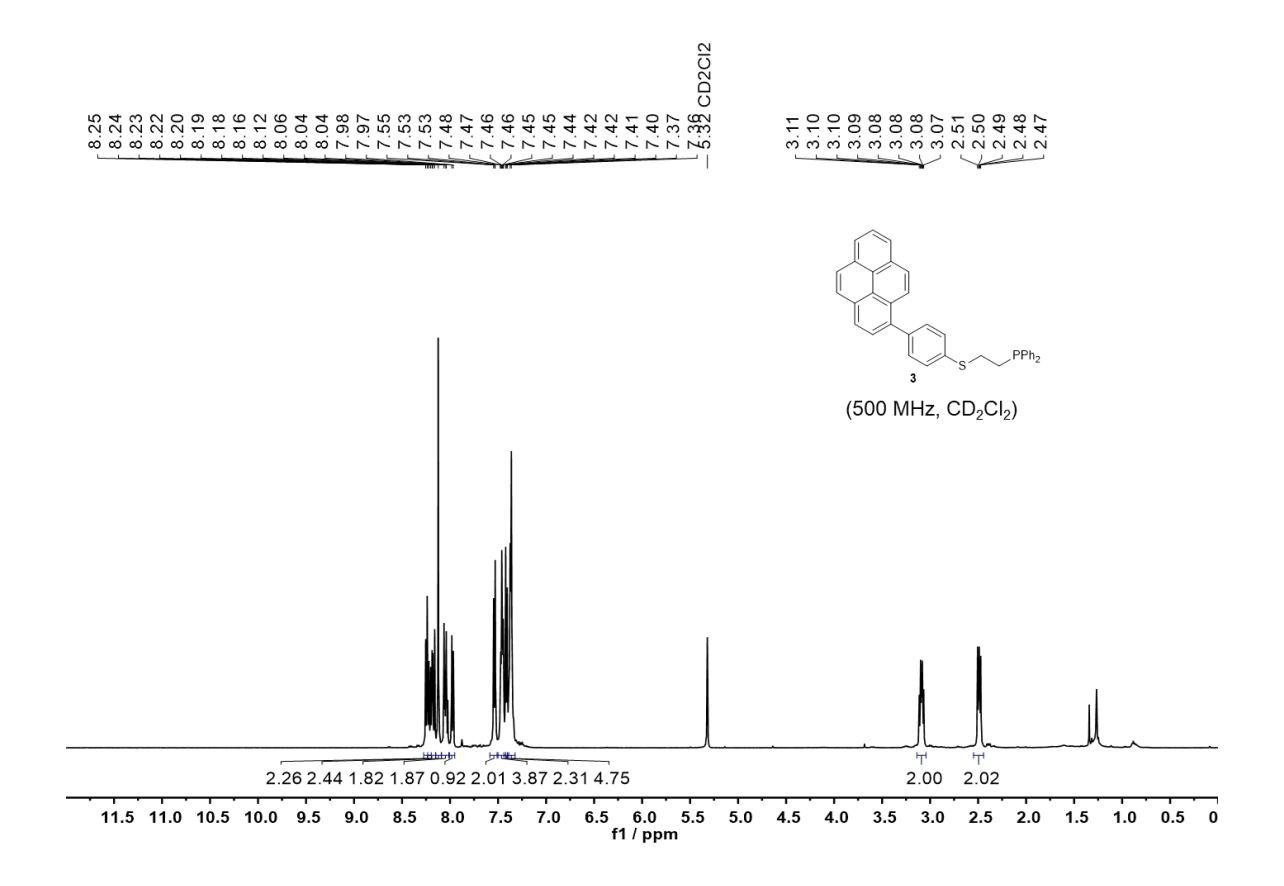




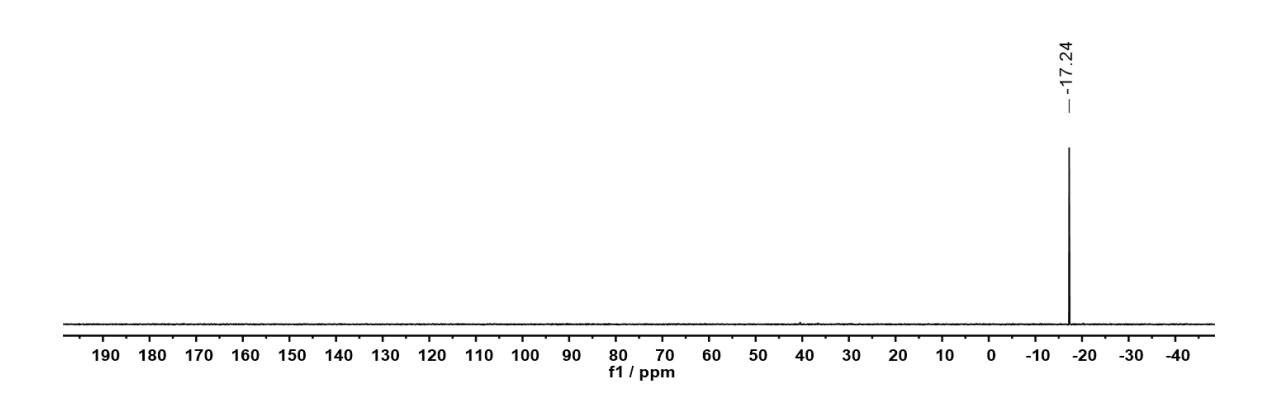


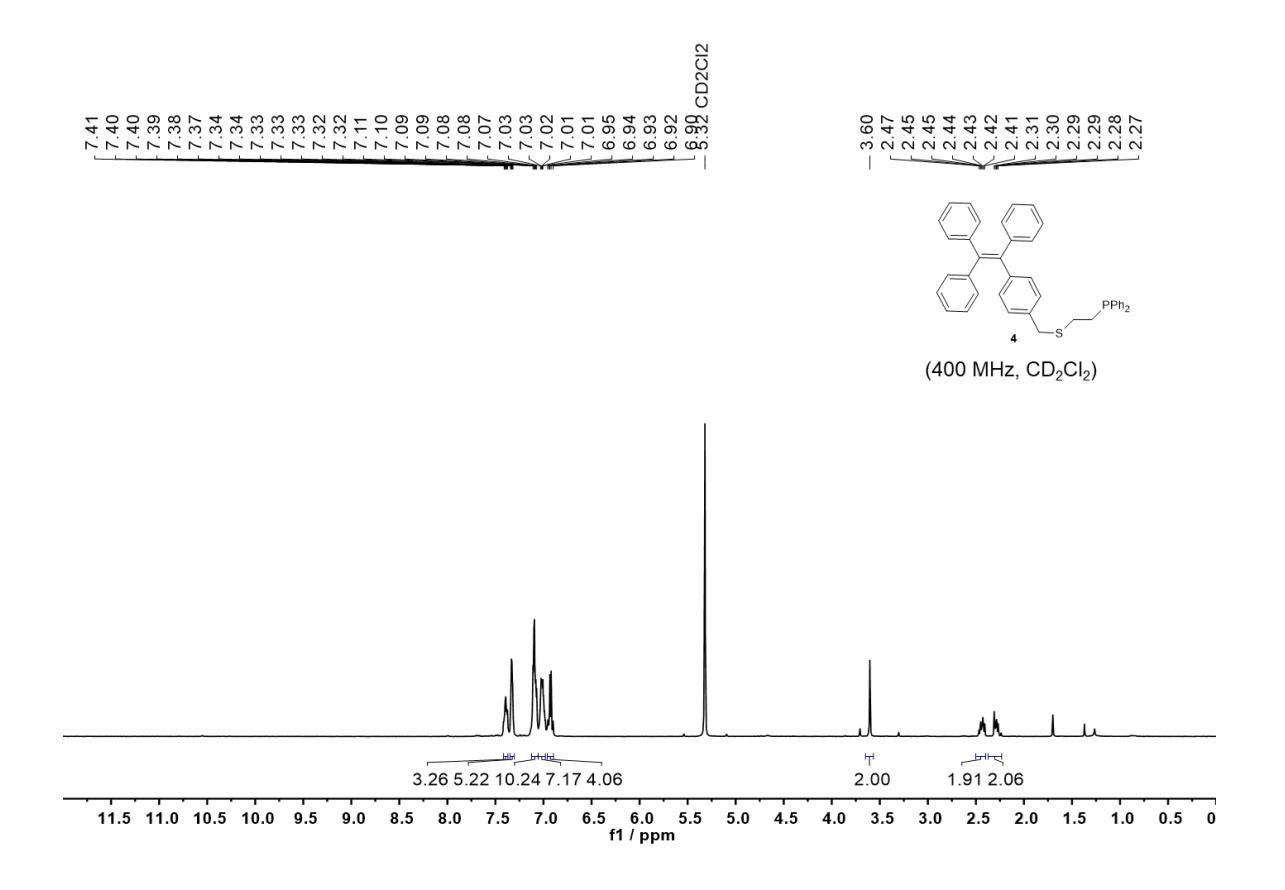


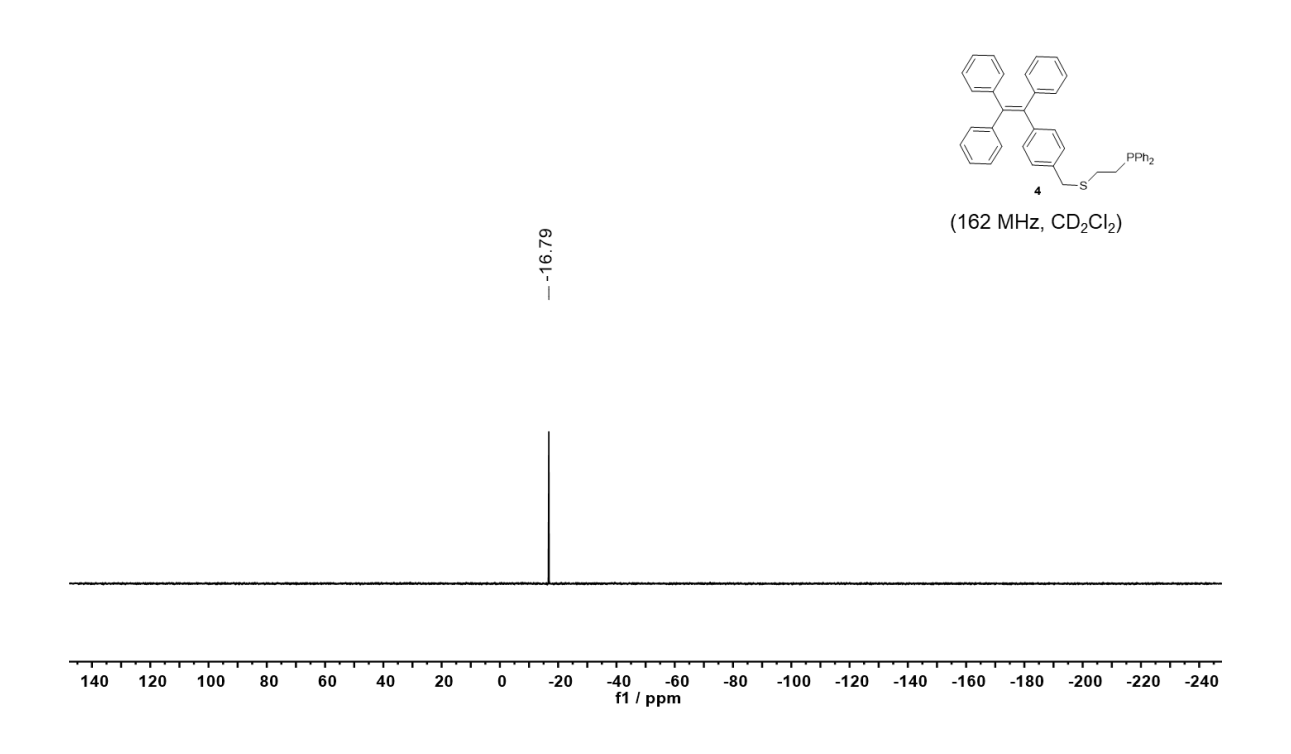


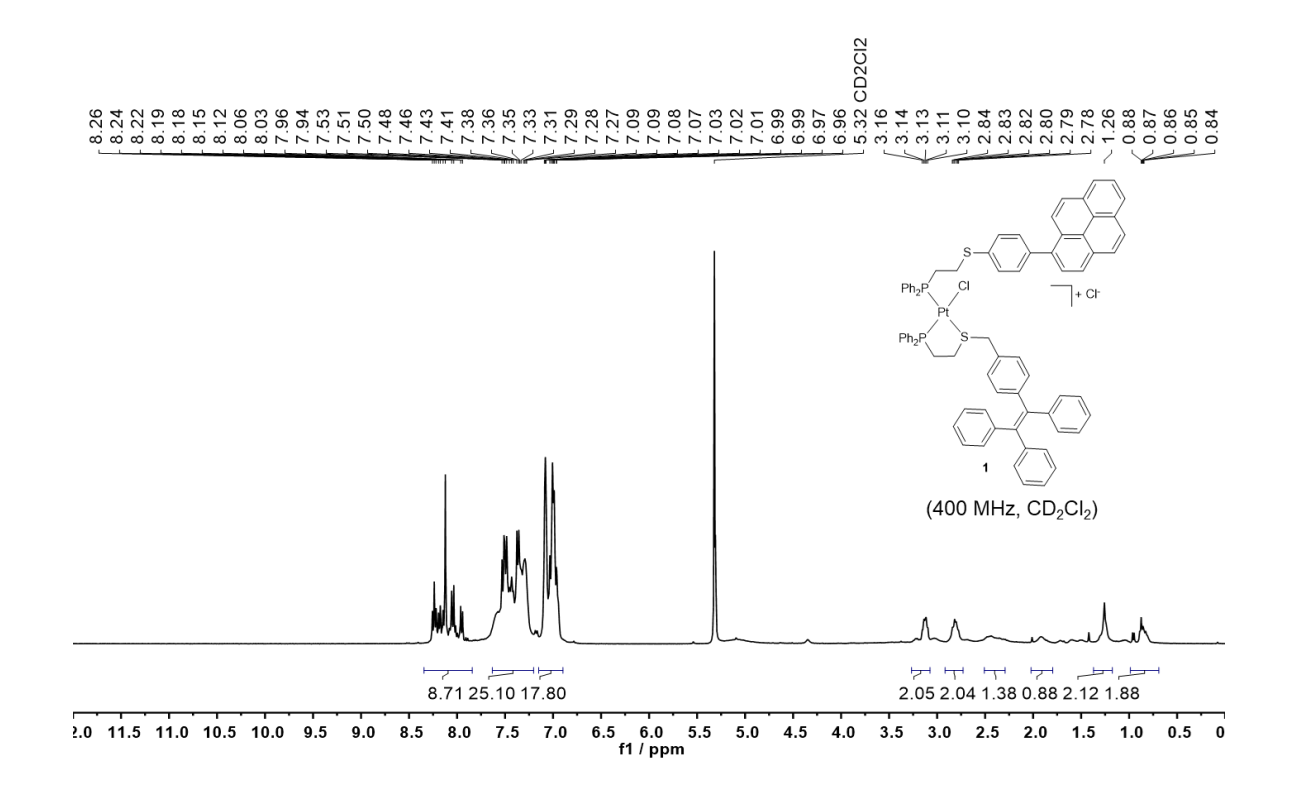


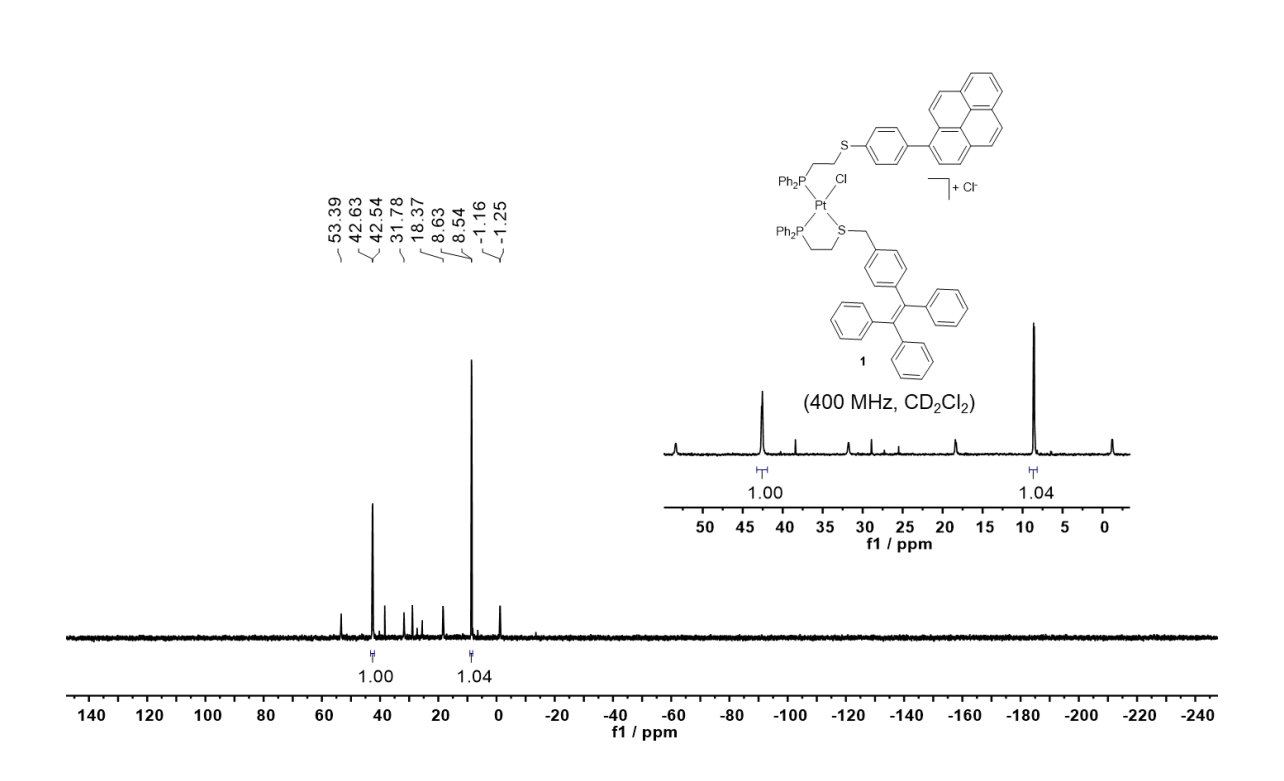


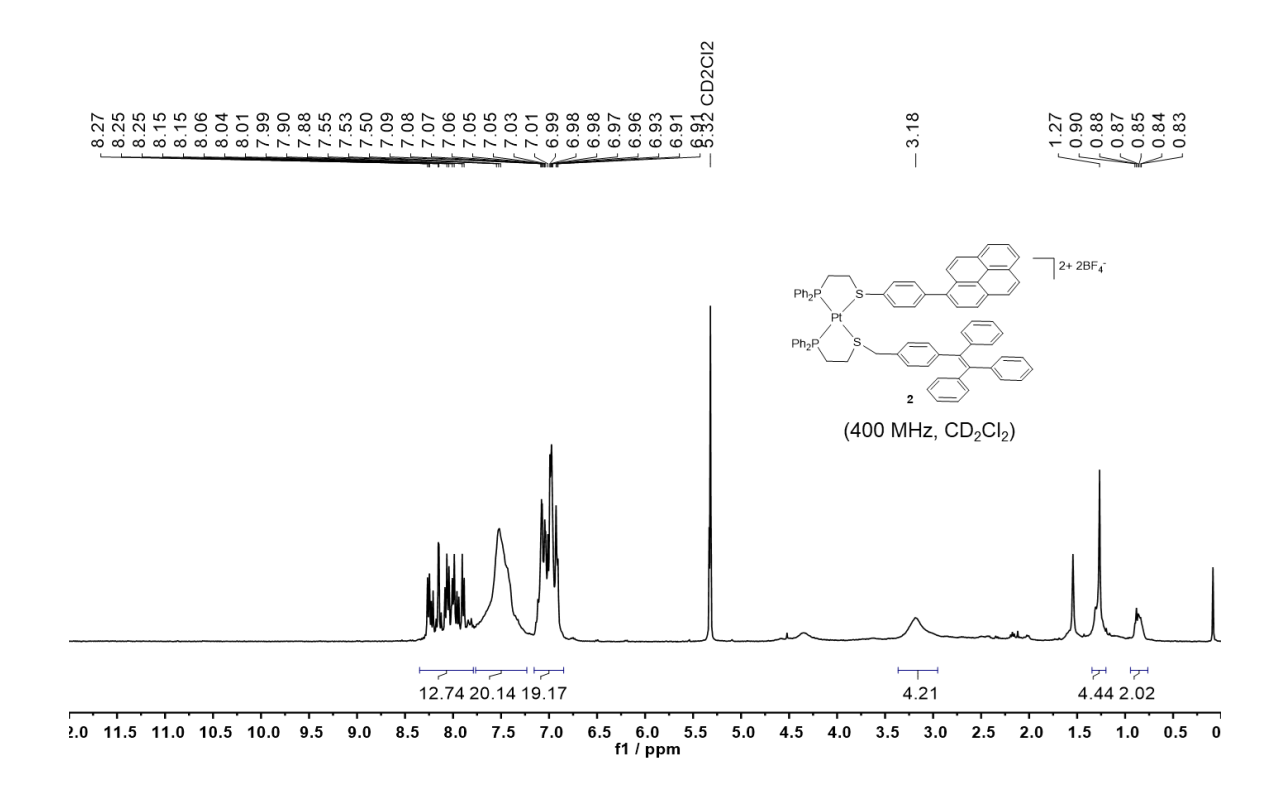


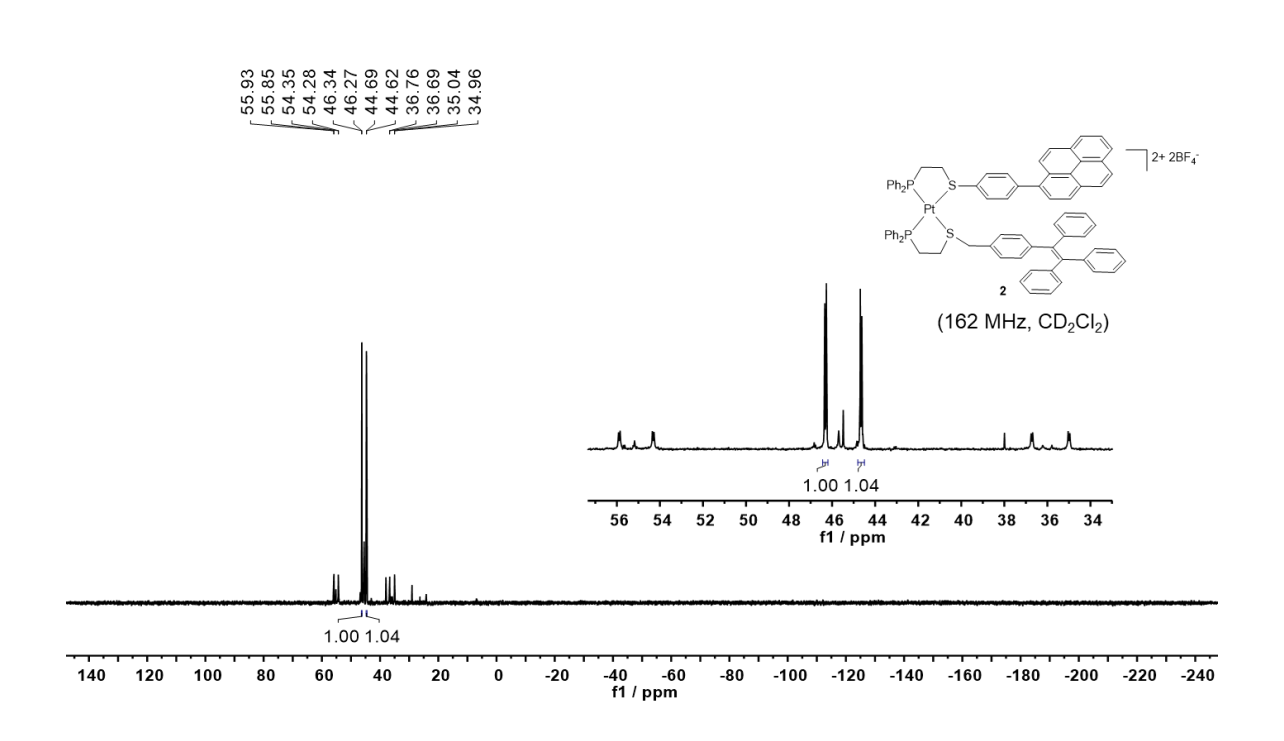


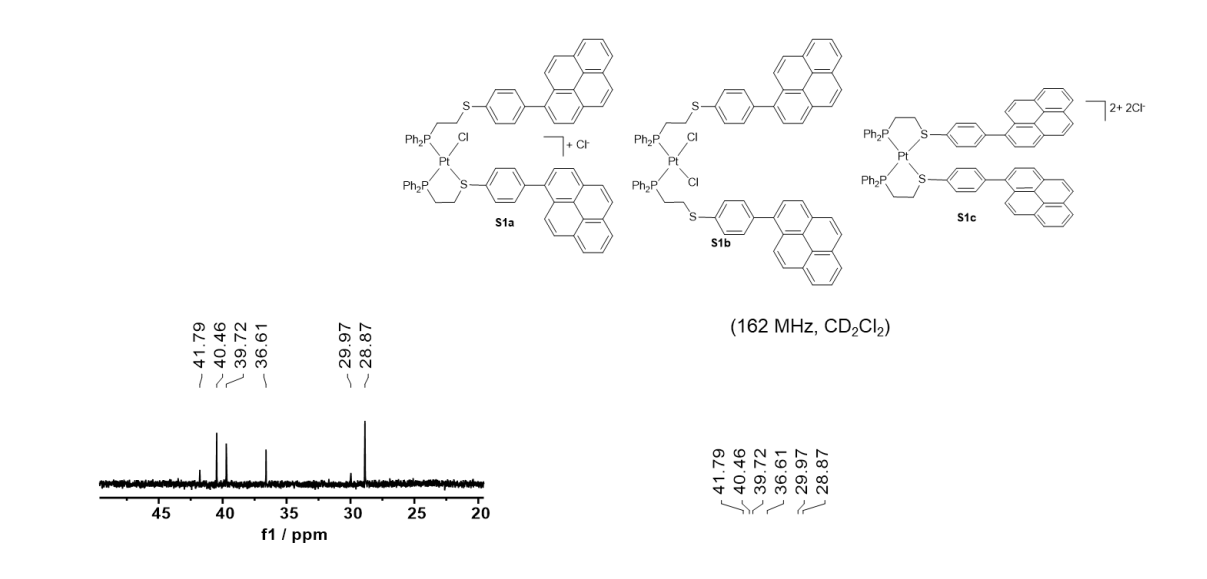


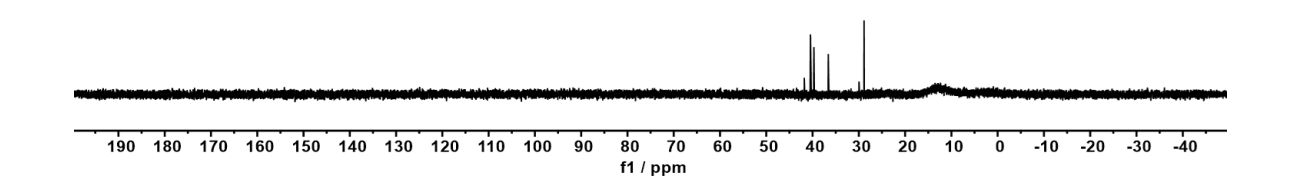




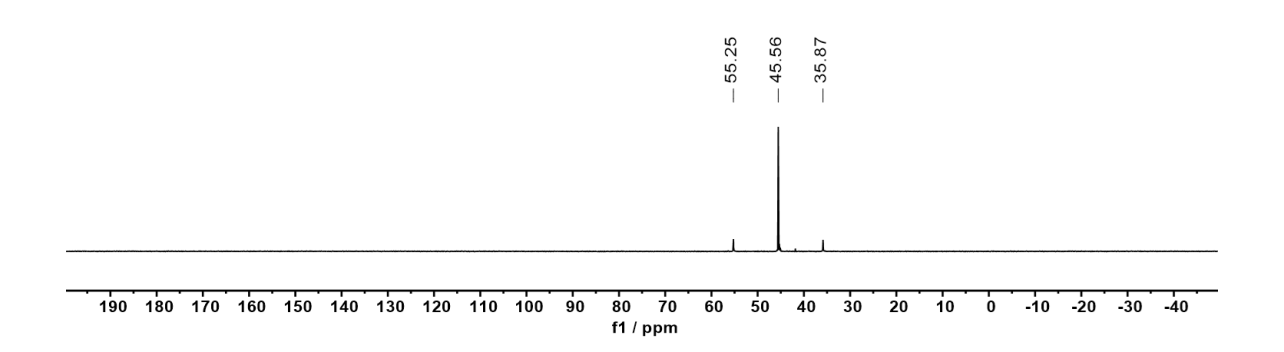


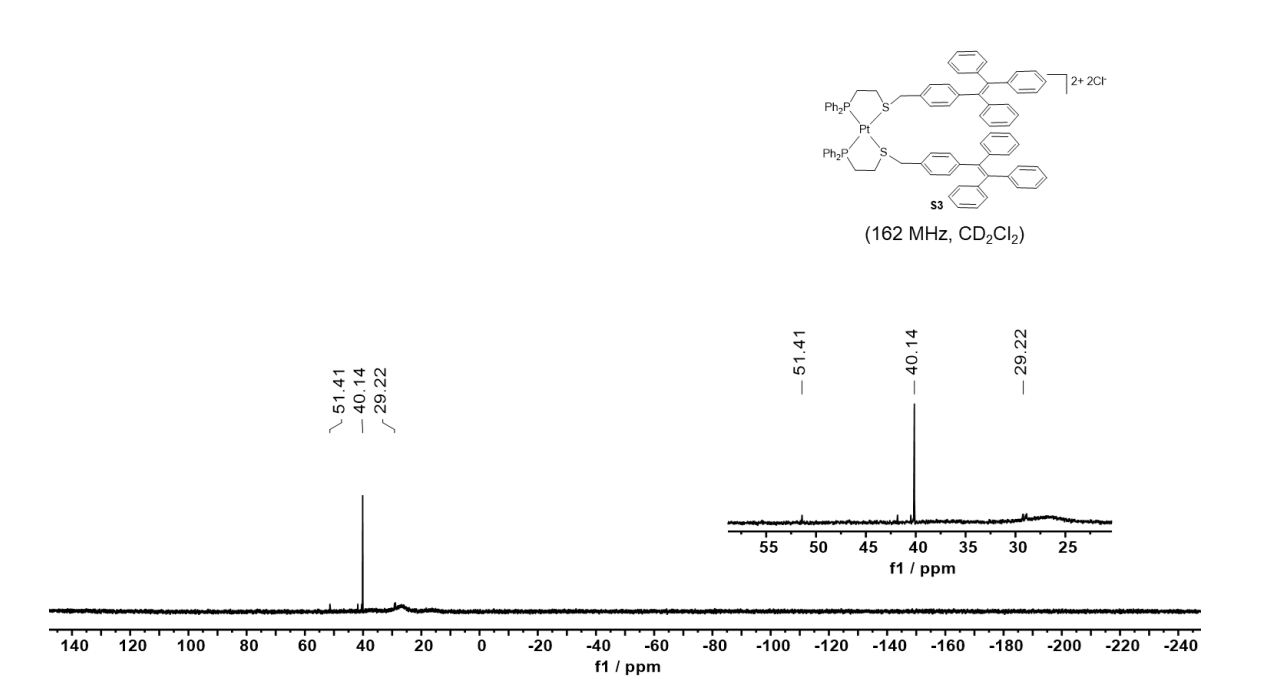












References

- 1 H. Shi, R. T. Kwok, J. Liu, B. Xing, B. Z. Tang and B. Liu, *J. Am. Chem. Soc.*, 2012, **134**, 17972.
- 2 H. J. Yoon, J. Kuwabara, J. H. Kim and C. A. Mirkin, Science, 2010, 330, 66.
- G. te Velde, F. M. Bickelhaupt, E. J. Baerends, C. Fonseca Guerra, S. J. A. van Gisbergen, J. G. Snijders and T. Ziegler, *J. Comput. Chem.*, 2001, **22**, 931.
- 4 C. Fonseca Guerra, J. G. Snijders, G. te Velde and E. J. Baerends, *Theor. Chem. Acc.*, 1998, **99**, 391.
- 5 SCM, ADF2017. http://www.scm.com
- 6 E. Van Lenthe and E. J. Baerends, *J. Comput. Chem.*, 2003, **24**, 1142.
- 7 J. P. Perdew, K. Burke and M. Ernzerhof, *Phys. Rev. Lett.*, 1996, 77, 3865.